# Mechanism of Training Induced Functional Gains and CST Sprouting after SCI: The role of PKA Signaling

by

David Zhihao Wei

A thesis submitted in partial fulfillment of the requirements for the degree of

Master of Science

Department of Neuroscience

University of Alberta

**Abstract**

Currently the most effective treatment in humans for promoting recovery after spinal cord injury (SCI) is rehabilitative training. However, training is not equally effective for all injury severities and usually does not lead to complete recovery. As a result, there is a need for treatments that can augment recovery in addition to training. One possible approach may be to first gain an understanding of how training promotes recovery. For example, animal studies of training induced recovery have previously found that motor recovery after spinal cord injury is associated with increased sprouting of the corticospinal tract (CST), a tract important for voluntary motor control. Increasing the activity of the secondary messenger cyclic AMP (cAMP) may also promote neurite sprouting and functional recovery in spinal cord injured rats. This occurs mainly through activation of the cAMP effector Protein Kinase A (PKA), as PKA inhibition prevents the growth promoting effects of increased cAMP activity *in vitro*. However it is currently unclear whether PKA inactivation also inhibits behavioral recovery. We hypothesized that increased cAMP-PKA signaling is necessary for CST sprouting and behavioral recovery after SCI, and inhibiting PKA signaling would inhibit these effects. We tested this possibility by infusing the PKA inhibiting compound Rp-cAMPS, through cannulation into the forelimb primary motor cortex (fM1) of partially C4 lesioned rats. Rats were then trained on the single pellet grasping (SPG) task for 4 weeks. At the end of training, and contrary to our hypothesis, we observed improved grasping success in the Rp-cAMPS treated group (Rp: 40.3 ± 5.4%, saline: 23.6 ± 5.7%, P=0.046), and increased CST sprouting into the grey matter rostral to the lesion compared to saline treated rats (Rp: 0.9 ± 0.2% fibers/mm, saline: 0.5 ± 0.08% fibers/mm, P=0.046). This recovery was not due to differences in lesion sizes (saline=22.3 ± 2.3%, Rp-cAMPS=26.7 ± 4.5%, P=0.41). However we did not detect a significant correlation between fiber sprouting and grasping success (r=0.06, P=0.82). We next searched for an alternative mechanism

that may account for the increased sprouting, and examined whether Rp-cAMPS affected inflammation. We observed no differences in the number of IBA1 expressing cells (a marker for microglia), or IBA1 expression in fM1 between groups. In conclusion, our results demonstrated that Rp-cAMPS infusion into fM1 improved grasping recovery and sprouting of the injured CST in rats. Because this is contrary to what is known about the function of PKA signaling, these results suggest more research is required to better understand the role of the cAMP signaling pathway in CST sprouting and behavioral recovery after SCI.

## Preface

This thesis is an original work by David Zhihao Wei. The research project, of which this thesis is a part, received research ethics approval from the University of Alberta Research Ethics Board, Project Name “Roles of cAMP and training in the recovery of reaching after spinal cord injury”, No. 254, Sept 2012 – June 2014.

**Acknowledgements**

For the completion of this thesis, I would like to express my gratitude to Caitlin Hurd, my predecessor on this project and wonderful lab mate. As well, I would like to thank Drs. Danny Galleguillos and Simonetta Sipione for technical assistance, my committee members Drs. Frederick Colbourne and Declan Ali for their support and insight, and my funding agency Canadian Institute for Health Research (CIHR) for providing the opportunity to pursue this experiment. Lastly, I would like to thank my ever-patient supervisor, Dr. Karim Fouad, for his guidance through the highs and lows of this project, and his encouragements and energy to see it to completion.

## Table of Contents

**List of Figures**

**Abbreviations**

ABC – Avidin/Biotin Conjugate

AKAR3 – A Kinase Activity Reporter 3

ANOVA – Analysis of Variance

BCA – Bicinchoninic Acid Protein Assay

BDA – Biotinylated Dextran Amine

BDNF – Brain Derived Neurotrophic Factor

cAMP – Cyclic AMP

CNG – Cyclic Nucleotide Gated Ion Channels

CNS – Central Nervous System

CREB – cAMP Response Element Binding Protein

CST – Corticospinal Tract

DAB – 3,3'-Diaminobenzidine

DLQ – Dorsolateral Quadrant lesion

EPAC – Exchange Protein Activated by cAMP

fM1 – Primary Forelimb Motor Cortex

FRET – Fluorescence Resonance Energy Transfer

GFAP – Glial Fibrillary Acidic Protein

IBA1 – Ionized Calcium-Binding Adaptor Protein 1

IL-6 – Interleukin 6

LPS - Lipopolysaccharide

MAG – Myelin Associated Glycoprotein

MEP – Motor Evoked Potential

Nogo A – Neurite Outgrowth Inhibitor, Isoform A

OMGp – Oligodendrocyte Myelin Glycoprotein

PDE IV – Phosphodiesterase, isoform IV

PKA – Protein Kinase A

pPKA – T197 Phosphorylated PKA Catalytic Subunit

RhoA – Ras Homolog Gene Family, Member A

RST – Rubrospinal Tract

SC – Sub-Cutaneous

SCI – Spinal Cord Injury

SPG – Single Pellet Grasp task

SEM – Standard Error Mean

TNF – Tumor Necrosis Factor

## 1. Introduction

*a. Spinal Cord Injury*

The spinal cord is an important neurological link between the brain and the rest of the body. It houses myelinated axons (white matter) surrounding the cell bodies of interneurons and motor neurons (grey matter). Motor signals from the brain and sensory inputs from the periphery travel via tracts in distinct regions of the white matter. At each level of the spinal cord, axons from ascending and descending tracts form primary or secondary connections to motoneurons in the grey matter and connect the central nervous system (CNS) to the periphery. Consequently, spinal cord injuries (SCI) may lead to sensory and motor deficits in all regions of the body innervated by the damaged tracts below the level of the injury. Depending on the severity of injury, permanent, partial or total functional loss may occur.

The quality of functional loss after SCI is dependent on the injury location. For example, damage to the cord at or below thoracic level commonly results in lower extremity impairments (paraplegia), while SCI at higher than mid-cervical levels affects functions in all four limbs (tetraplegia). The occurrence of tetraplegia is most common, accounting for over 50% of new SCI cases each year, although in most cases these individuals are left with some residual functions (reviewed in Sekhon & Fehlings, 2001; National Spinal Cord Injury Statistics Center, NSCISC 2014). The high incidence of cervical injuries may be due to the fact that cervical segments are less stabilized by muscles and ligaments, and are easily damaged during high-energy impacts involved in traumatic SCI (NSCISC 2014; Sekhon & Fehlings, 2001). This correlates with the finding that the incidence of SCI is highest in the 20-30 years old age group, as young adults are most likely to participate in activities resulting in SCI (Van den Berg et al., 2010). Acute mortality rates after SCI may be as high as 80%, but life expectancies for individuals who survive the first year are, on average, not dramatically different from the uninjured population (Sekhon & Fehlings, 2001; NSCISC 2012).

Despite the long-term survival of people with SCI, functional deficits usually remain over an individual's lifetime. This persistence of deficits is related to the inability of CNS neurons to regrow. Although compensatory mechanisms, such as neurite sprouting (or plasticity) from spared fibers exist in the CNS, the resulting recovery is usually incomplete. These chronic motor deficits can drastically affect an individual's quality of life, and numerous studies suggest that motor recovery is among the priorities for people with SCI (Westgren & Levi, 1998; Anderson, 2004; Simpson et al., 2012). This is especially true for tetraplegics, who highly rank the restoration of arm and hand functions as a goal for improved quality of life (Anderson, 2004), thus providing an important aim for SCI research.

Two broad areas of research for potential treatments that restore function include minimizing secondary damage and promoting neurite growth in the damaged cord. Minimizing secondary damage focuses on reducing the delayed tissue damages that occur following the initial injury. Promoting neurite growth examines ways to encourage greater functional recovery after SCI through increased growth and repair of damaged neuronal connections. This latter area was the focus of the current study, and was investigated using a rat model of incomplete tetraplegia. We investigated the sprouting of the corticospinal tract (CST), the main tract involved in fine motor control after injury, and examined how PKA (Protein Kinase A) activation affected CST sprouting and motor recovery. The next sections will first discuss the role of the CST in motor control, and how reorganization occurs in this pathway after injury, before detailing how PKA may be critical for these processes.

*b. Motor Control and the Corticospinal Tract*

The spinal cord is involved in motor control in several ways, including hosting intraspinal neuronal networks and motoneurons that may independently generate oscillatory movements, and gating spinal reflexes. But its primary function within the motor system is to serve as a conduit through which multiple brainstem nuclei and neocortical projections travel to their target neurons. These projections orchestrate various aspects of movement, both voluntary and involuntary. The most important descending tract is the CST, which controls movement through direct and indirect activation of motor neurons in the anterior horn of the spinal grey matter (reviewed in Lemon, 2008). Rare instances of SCI resulting in focal loss of the CST demonstrate that patients with disruptions of connections in this tract suffer from acute paralysis and chronic disturbances of motor control (Nathan, 1994; Lemon & Griffiths, 2005). These cases demonstrate that although the CST is important for motor control, even total loss of CST input does not lead to permanent paralysis, and recovery of motor function is still possible. How recovery may occur at the neuronal level in the damaged CST will be the topic of the following section.

*i. Anatomy and Function of the CST*

The main function of the CST is to orchestrate movement, so it both receives inputs and contains outputs from a variety of cortical areas to serve this purpose. Inputs to the CST integrate both sensory and motor information from areas of the neocortex, striatum, thalamus, and cerebellum to govern movement. Resulting outputs are projected from several motor cortical areas in the frontal lobe, including the primary, supplementary, and premotor cortices, but outputs also contains a small amount of somatosensory projections. The tract's cell bodies are pyramidal neurons that reside in layer V of these cortical areas. In both rodents and humans, the majority of CST projections decussate at the medullary pyramids to innervate spinal motoneurons in the contralateral half of the cord. Two small portions of alternative projections also exist. The first of these do not decussate, and

instead continue down the cord to form ipsilateral connections. Another small portion decussates but travels in distinct regions from the main tract (ventral and anterior for rats and humans respectively). These alternative projections are involved in modulating gross motor movements (Lacroix et al., 2004), but also have important roles in recovery, as will be discussed. As CST projections travel down the cord, axon extensions from the main tract form mono- or polysynaptic connections with motoneurons in the ventral horn of the grey matter. Motoneuron pools also extend through the length of the cord, and two regions of the cord have especially large clustering of motoneurons. These are the cervical enlargement (segments C3-C7) that contain motoneurons innervating shoulder, arms, and hand muscles, and the lumbar enlargement (L1-S2) that innervate muscles of the lower limbs. In addition, the CST has branches to several brainstem motor nuclei, including the raphe nucleus, nuclei of the reticular formation, as well as the red nucleus (Esposito et al., 2014; Z'Graggen et al., 2000). These inputs may be referred to distinctly as the corticobulbar tract, and gives the CST indirect control of brainstem mediated motor functions such as balance and gating of reflex controls (reviewed in Isa & Nishimura, 2014).

One of the central roles of the CST is fine motor control, which is necessary for detailed coordinated movements such as grasping with the hand and fingers. Humans have a small, but significant portion of direct cortico-motoneuronal connections that are responsible for our dexterous hand functions. Rat CST projections contact interneurons in the intermediate laminae of the cord, and their lack of monosynaptic connections results in less independent finger movements (Heffner & Masterton, 1975; Yang & Lemon, 2003). Yet like their human counterparts, rats' grasping abilities are nonetheless affected by CST ablations. For example, following CST damage, rats may demonstrate increased errors in targeting when reaching for objects; less coordinated forelimb and paws movements; and decreased ability to manipulate objects with their paws compared to uninjured controls (Whishaw et al., 1998; Kanagal & Muir, 2007). Furthermore, some recovery of functions may

occur, but these recoveries are rarely complete, and rats with CST damage display long-term deficits in paw use (Wang et al., 2011).

*ii. CST and Recovery of Motor Functions after Injury*

After SCI, adaptive growth occurs in multiple spinal tracts and may correlate with functional recovery. These adaptive processes have been demonstrated at all levels of the CST, and examples of these processes include sprouting of injured and uninjured fibers to form new connections, and synapse remodeling (Fouad et al., 2011; Onifer et al., 2011). To demonstrate the effectiveness of these new connections, Krajacic et al. (2010) trained rats on a task until they demonstrated significant recovery following a CST lesion, then performed a second lesion at a more rostral position in the cord. They observed the elimination of training induced recoveries after the second lesion, which may be suggestive that the rostral CST reformed connections after SCI. A separate study by Fouad et al. (2001) provided more direct evidence that the CST reforms connections to distal targets separated by a lesion. In this study, the authors stimulated the motor cortex after CST lesions, and demonstrated the return of evoked motor potentials in initially unresponsive distal muscles over time. Several hypotheses exist to postulate how these changes facilitate motor recovery, including detour formation of the injured CST and compensation involving uninjured tracts. The first of these, detour formation, occurs when injury induced neuronal sprouting bypass the lesion site by forming alternative pathways. For example, new sprouting may contact propriospinal interneurons that extend regionally in one or several spinal segments to reconnect to caudal targets (Bareyre et al., 2004; Vavrek et al., 2006).

Beyond detour formation, there are other methods of CST rewiring that may provide functional compensation after SCI. For example, the spared CST may take over functions of the injured CST after SCI. This process may occur through either spared ventral CST projections directly contacting denervated motor neurons (Weidner et al., 2001), or sprouting of the contra-lesional CST into the grey matter to strengthen ipsilateral connections to denervated motoneurons (Brus-Ramer et al.,

2007). As well, changes at the level of the motor cortex may also be implicated in recovery. The motor cortex is generally organized into motor maps, with the activation of different cortical areas triggering movement of specific body parts. After SCI, there is a loss of motor map representations of body parts that have been denervated by the injury. Treatments that prevent or delay these map losses, such as by forcibly activating motor maps through grasping training, also may be associated with functional recovery (Girgis et al., 2007).

In addition to changes within the CST during recovery, there are also adaptive changes occurring in brainstem tracts involved in motor control. In rats, for example, functional recovery is associated with plasticity involving the rubrospinal tract (RST), a brainstem motor tract originating from the red nucleus. Similar to the CST, this tract also decussates at the level of the brainstem to innervate motoneurons of the contralateral body. Although the RST mostly projects to the intermediate laminae of the grey matter in rats, evidence suggests that it additionally has direct motoneuronal contacts onto motoneurons of distal forelimb muscles (Kuchler et al., 2002). This suggests the RST has an important role in grasping control for rats, and is suited to compensate for motor deficits after CST damage. Indeed, selective RST ablations results in grasping deficits (Whishaw et al., 1998; Muir et al., 2007), and CST ablations may be followed by RST fibers growing into grey matter areas originally innervated by the CST (Raineteau et al., 2002). An informative study by Z'Graggen et al. (2000) underlines the importance of the RST in functional compensation after SCI in rats. First, the authors demonstrated that in pyramidotomized neonatal rats, forelimb muscle reinnervation, indicated by a return of MEPs is associated with CST projections growing toward the red nucleus. Second, pharmacologically suppressing activity in the red nucleus abolishes restored MEPs in response to motor cortex stimulation. These studies provide evidence that motor recovery is not solely CST dependent in rats, and adaptive changes may occur in other descending motor tracts to synergistically provide functional recovery after SCI.

*iii. Examining Motor Deficits and Recovery Using Rehabilitative Training after SCI*

Currently the most effective treatment for motor recovery after SCI is rehabilitative training. For tetraplegics, this involves reaching and object manipulation using the hands. Such behavior is modeled in rats using activities requiring skilled grasping, such as the single pellet grasping task (SPG). In addition to being clinically relevant, benefits of using SPG include the possibility to finely assess movement deficits after an injury (Whishaw et al., 1998). As well, grasping (as compared to walking) depends on a relatively straightforward neuronal network, involving the motor cortex to motor neurons and muscle output. In addition, the major CST projections in rats travel dorsally, allowing easy surgical access to the tract in studies examining grasping. Thus, adaptive changes within this pathway in response to grasping training are accessible for study. Based on these reasons, we utilized SPG training in rats after CST injury to study the mechanisms of recovery after SCI.

It is clear that neurite sprouting plays a major role in recovery after SCI, but it is currently unclear what the molecular mechanisms responsible for sprouting are. Further understanding of these mechanisms will be essential if we were to increase sprouting as a treatment target to promote functional recovery.

*c. The Nitty-Gritty: Using PKA to Facilitate Adaptive Neuronal Changes after SCI*

Current therapies that promote neurite sprouting and functional recovery after SCI are limited in their efficacy. For example, rehabilitative training has a window of efficacy that diminishes with time delays between injury and the start of training (reviewed in Fouad & Tetzlaff, 2012). Since SCI patients usually require weeks of physical recuperation after the major trauma, it is unrealistic for many to undergo training when it would be most beneficial. Thus there is this potential to increase training efficacy for many patients. At the neuronal level, this diminishing recovery is exacerbated by a variety of factors that suppress neurite growth in the adult spinal cord. These growth suppressors include the astrocytic scar, myelin associated inhibitors, as well as a lack of growth promoting factors. Training may initially overcome some of these growth-suppressing conditions, but the decline of training efficacy also suggests an underlying decrease in training's ability to initiate adaptive changes over time.

To boost training efficacy, research has been devoted to finding a treatment that may prolong and boost training induced neurite sprouting. A successful treatment may be required to overcome multiple growth suppressing factors, as each of the above mentioned factors are potent inhibitors of neurite sprouting alone. One potential target is to increase PKA activation in the cAMP (cyclic AMP) signaling pathway, as pharmacological activation of this enzyme is able to facilitate neurite sprouting both *in vitro*, within a growth inhibitory environment composed of myelin inhibitors (Cai et al., 1999), as well in rats after SCI (Nikulina et al., 2004). Furthermore, increased PKA activation is associated with increased growth promoting activity of other growth factors, as well as with training itself. The next sections will discuss the role of cAMP-PKA signaling in promoting neurite sprouting and mitigating various growth inhibiting factors after SCI.

*i. cAMP as Mediator of Training Dependent Neurite Sprouting*

One of the driving signals of cAMP production is neuronal activity. In response to increased neuronal activity during training, cAMP production is also increased through activation of $Ca^{2+}$ dependent adenylyl cyclase. In addition, increasing neuronal activity drives the expression of neurotrophins important for neurite sprouting, including Brain Derived Neurotrophic Factors (BDNF). BDNF signals mainly through binding to Tyrosine Receptor Kinase B, resulting in the activation of signaling cascades involved in neuronal survival and growth. Specifically, exercise induced muscle activation increases motoneuron BDNF levels proportional to the amount of exercise undertaken by rats (Gomez-Pinilla et al., 2002). And increased BDNF expression promotes fiber sprouting in adult rat spinal cords after SCI (Zhou & Shine, 2003). Conversely, blocking BDNF expression during training also blocks the beneficial effects of training on recovery after CNS injury in rats (Ploughman et al., 2009). *In vitro*, BDNF is an attractant signal for neurite growth cone turning. However, inhibiting PKA activation in neurites presented with a BDNF gradient change this attractant signal to repulsion (Song et al., 1997). This suggests that BDNF may partially exert its effects through activation of the cAMP-PKA pathway. Indeed, BDNF indirectly inhibits the cAMP degrading protein Phosphodiesterase IV (PDE IV), leading to increased intracellular cAMP levels with increased BDNF activity (Gao et al., 2003, Figure I. VI).

*ii. cAMP Negates the Inhibitory Effects of MAG on Neurite Sprouting*

Myelin is produced in the CNS by oligodendrocytes, and its main functions are to ensheath the axon and facilitate axon signal propagation. After SCI, distal axons degenerate and leave behind their myelin sheath. Following myelination during development, myelin sheaths and myelin fragments are growth inhibitory, and in an injured cord become a major roadblock to regrowth by forming a repellent barrier to sprouting neurites that approach it. The growth inhibition occurs when regrowing axons contact myelin, and exposed myelin associated proteins trigger signaling cascades leading to growth

cone collapse. Three main classes of myelin associated growth inhibitory proteins are currently identified. These are Myelin Associated Glycoprotein (MAG), Oligodendrocyte Myelin Glycoprotein (OMGp), and Neurite Outgrowth Inhibitor (Nogo). Each of these classes of proteins has different regions of expression on the myelin surface. For example, Nogo A is the most heavily expressed Nogo isoform in the CNS (Huber et al., 2002), and is present on the innermost loop of the undamaged sheath, where it has direct contact with axons. MAG is also found mostly on the innermost loop of CNS myelin, where it may directly contact axon surface receptors. OMGp on the other hand, does not seem to have high levels of expression on CNS myelin, but is still a potent inhibitor of neurite outgrowth (reviewed in Filbin, 2003).

Despite the reported role of myelin as growth inhibitory, researchers have observed that cultured spinal neurons extracted from neonatal rat pups do not display inhibited neurite extension when grown on adult myelin (Cai et al., 2001). This suggests a more complicated involvement of myelin proteins in neurite growth than simple inhibition. Furthermore, it suggests that identifying the factors that allows young neurons to grow on myelin may provide a treatment that facilitates growth by restoring the injured spinal cord to a more developmental like stage. One proposed factor is cAMP, as previous experiments suggest that cAMP levels govern the effect of MAG on neurite outgrowth. For example, Song et al. (1998) studied the effect of exposing cultured *xenopus* spinal neurons to MAG gradients. They found that pretreatment with a cAMP analogue resulted in neurites growing toward the gradient instead of away. A similar experiment performed by Cai et al. (1999) used rat spinal neurons cultured on a layer of MAG expressing cells. These authors reported that MAG exposed neurons increased sprouting to levels comparable to control cells if they were pretreated with BDNF or a cAMP analogue. Conversely, inhibiting PKA with the inhibitory cAMP analogue Rp-cAMPS (Rp) also inhibited neurite extension of neonatal neurons on MAG, so that neonatal neurons exhibited similar levels of growth on MAG as adult neurons (Cai et al., 2001; Fig 1. VII).

In addition to the effect of cAMP on MAG, the secondary messenger may also act on other myelin associated inhibitors to promote neurite sprouting. For example, a recent study by Sepe et al. (2014) demonstrated that activation of the cAMP-PKA pathway may result in the direct degradation of Nogo A, which also leads to increased neurite sprouting of cultured neurons. There may also be a broader effect of cAMP on myelin inhibitors through inhibition of the protein Ras Homolog Gene Family Member A (RhoA). RhoA is a downstream target of myelin inhibitors that is involved in cytoskeleton stabilization, and its activation prevents the cytoskeletal reorganization required for neurite sprouting. Although PKA inhibition of RhoA is reported in many cell types, it is currently unclear whether this process occurs in neurons (reviewed by Howe, 2004). Nonetheless, one of the mechanisms of cAMP mediated neurite sprouting involves attenuation of the growth inhibitory effects of myelin inhibitors.

*iii. cAMP and Glial Scarring*

Glial cells respond to traumatic injuries such as SCI by forming a scar around the injury site. The biggest component of scarring is reactive astrocytes, which are distinguished from resting state astrocytes by excessive expression of the intermediate filament Glial Fibrillary Acidic Protein (GFAP). Reactive astrocytes at the injury site also upregulate secretion of proteoglycans, forming physical and biochemical barriers to extending neurites (reviewed in Maier & Schwab, 2006). Digestion of proteoglycans by proteases has been demonstrated to have positive effects on neurite outgrowth in rats after SCI (Cafferty et al. 2007), and may lead to functional recovery if combined with training (Garcia-Alias et al., 2009).

Another component of the glial scar are microglia. These resident immune cells are vital for housekeeping functions such as maintaining synaptic integrity within the CNS. As a result of the intense inflammatory signal after SCI, microglia increase expression of the specific marker Ionized calcium-Binding Adapter molecule 1 (IBA1; Ito et al., 1998) and release reactive oxygen and nitrogen

species that promote oxidative damage. Additionally, they up-regulate pro-inflammatory cytokines such as Tumor Necrosis Factor (TNF), which activate cell death signaling and recruit peripheral immune cells to the injury site to exacerbate secondary damage (reviewed in David & Kroner, 2011). Increasing intracellular cAMP levels is linked to the attenuation of this inflammatory response and may reduce the amount of secondary damage that occurs as a result of increased TNF expression. For example, administering a cAMP analogue to cultured microglia *in vitro* resulted in decreased TNF expression (Woo et al., 2003). Furthermore, rats receiving treatments that elevate cAMP levels after SCI exhibited decreased levels of TNF in addition to improvements in neurite sprouting (Pearse et al., 2004). In a separate study, authors Atkins et al. (2007) used a rat traumatic brain injury model to study the effects of cAMP elevation on TNF expression and injury size. Their results suggest that continued administration of the cAMP elevating drug rolipram beginning immediately before injury resulted in reduced TNF levels and reduced injury sizes. Thus increasing cAMP levels may also promote recovery through attenuation of inflammation and reduction of secondary damage after SCI.

In contrast to the view that inflammation is harmful after SCI, there has been a focus on the neuroprotective and regenerative role of macrophages in recent years. For example, microglia recruitment to the injury site may also be neuroprotective by forming a barrier between injured and healthy tissue (Loane & Byrnes, 2010; David & Kroner, 2011). In addition, macrophages may secrete a variety of growth factors that are essential for neuron survival, including pro-survival interleukins, BDNF, NT3, and NT4 (London et al., 2013; Donnelly & Popovich, 2008). Increasing the inflammatory response may thus be beneficial, as Rapalino et al. (1998) demonstrated that grafting activated peripheral macrophages after SCI promotes motor recovery and axon growth. These contradictory effects of inflammation seem to depend on the time course of microglia recruitment, where initial infiltrating microglia cause tissue damage and pro-survival microglia phenotypes are recruited days to weeks after the injury (Loane & Byrnes, 2010). Although it is currently unclear what the long term effects of cAMP-PKA activation may be on microglia phenotypes, prior experiments demonstrating

PKA suppression of TNF expression, alongside experiments demonstrating PKA mediated expression of the pro-survival interleukin-6 (IL-6), suggest increased PKA activity may increase the activity of pro-survival microglia phenotypes and neuronal regrowth (reviewed in Hannila & Filbin, 2008).

*iv. PKA and Recovery after SCI*

PKA is a tetrameric member of the AGC (Protein Kinase A, Protein Kinase G and Protein Kinase C) family of proteins. The common characteristics of this protein family include regulation of catalytic activity by phosphorylation. PKA is composed of two regulatory subunits bound to its catalytic subunits at resting state, and its activation requires the binding of two cAMP molecules to each regulatory subunit. Upon activation, phosphorylated PKA catalytic subunits (pPKA) dissociate from the regulatory subunits, and phosphorylate downstream targets in various cellular compartments, including the nucleus (Gervasi et al., 2007). Phosphorylation of the nuclear target transcription factor cAMP Response Element Binding protein (CREB) increases the expression of growth related genes necessary for neurite sprouting (Gonzalez & Montminy, 1989; Fig 1. I-V).

In addition to PKA, the secondary messenger cAMP has several other downstream targets, including Cyclic Nucleotide-Gated ion channels (CNGs), and Exchange Proteins Activated by cAMP (EPAC). However our experiment focuses on PKA because the majority of past research examining the role of cAMP signaling in neuronal sprouting has focused on PKA as the main downstream target. These previous studies have demonstrated that PKA activation is involved in multiple mechanisms of plasticity, from neuronal long term potentiation and synaptic plasticity (Impey et al., 1998; Chheda et al., 2001; Chain et al., 1999) to neuronal sprouting induced by pharmacological PKA activation in an inhibitory environment or after spinal lesions (Cai et al., 2001; Cao et al., 2006; Aglah et al., 2008).

PKA activity is affected by SCI, as levels of both cAMP and pPKA are suppressed in the CST for several weeks after injury (Pearse et al., 2004; Krajacic et al., 2009). SCI studies examining

increased PKA activation through cAMP suggests that elevating cAMP levels in rats, either by itself or in combination with other treatments, increased motor fibers sprouting and functional recovery after treatment (Nikulina et al., 2004; Pearse et al., 2004). As well, Macdonald et al. (2007) reported that combining training with a cAMP elevating treatment is more efficacious than training alone at promoting grasping recovery in rats after motor cortex injury. This suggests that pharmacological PKA activation may be used in combination with training to increase recovery after SCI.

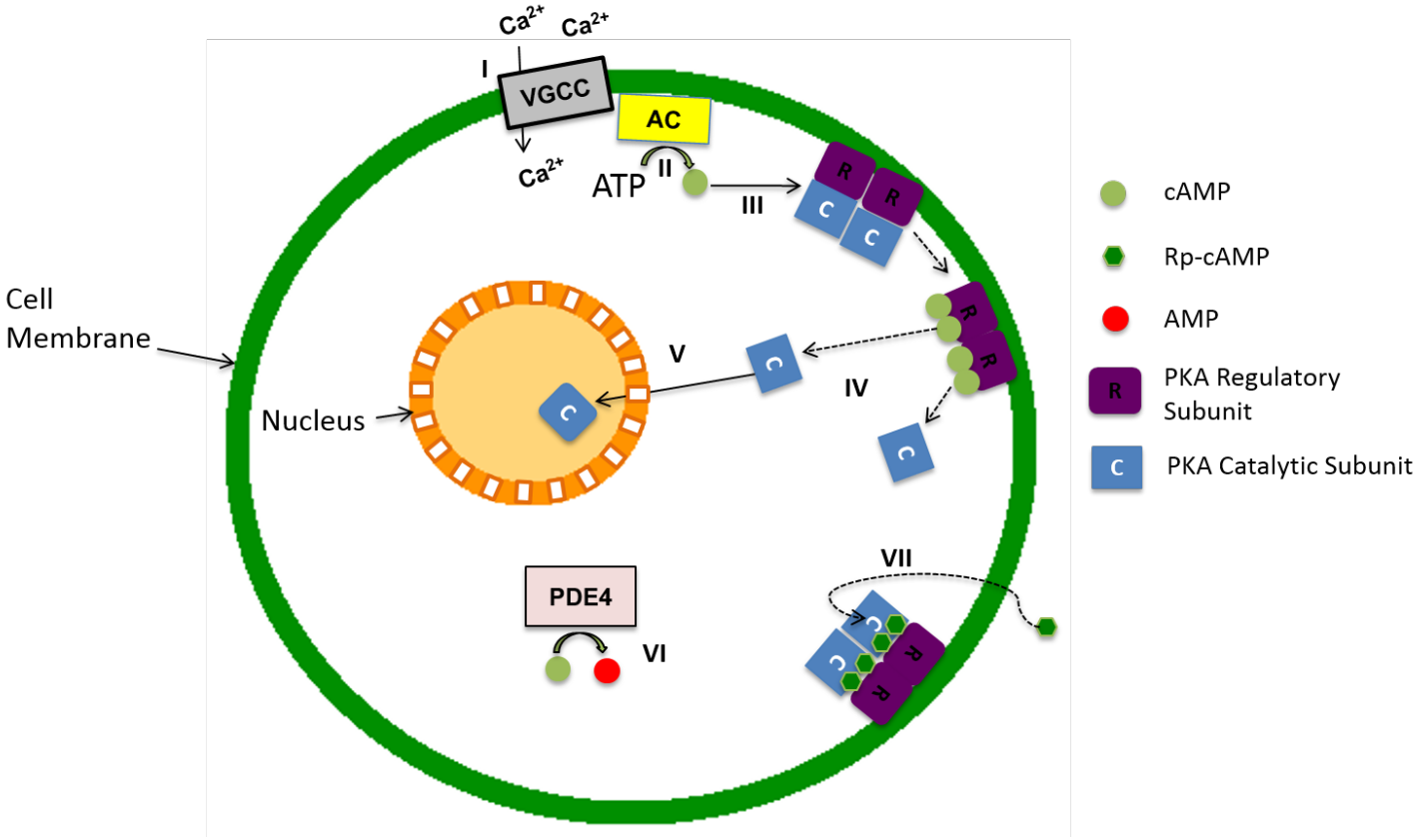


**Figure 1. The cAMP-signaling pathway.** (**I**) Upstream signals trigger increased cAMP production by adenylate cyclase (**AC**). (**II**). cAMP binds to PKA regulatory subunits (**III & IV**), leading to the nuclear translocation of its catalytic subunits through diffusion (**V**), and increased expression of growth promoting factors. PKA activity can be inhibited through either cAMP breakdown into AMP by phosphodiesterase IV (**VI**), or blockade of cAMP binding to PKA by pharmacological inhibitors such as Rp-cAMPS (**VII**).

*d. Experimental Design*

The purpose of the current study was to examine whether PKA activation is crucial for training induced grasping recovery and CST sprouting after SCI. Answering this question may allow researchers to design combination treatments that improve the functional gains of rehabilitative training by simultaneously increasing PKA activity. To test the role of PKA, we modeled SCI using a dorsolateral quadrant lesion (DLQ), and combined this with the SPG task, a combination that has been used successfully in our laboratory to test for SPG training induced recovery (Hurd et al., 2013). To tease out the effects of PKA in grasping recovery, we simultaneously inhibited PKA activation using the specific PKA inhibitor Rp-cAMPS injected through cannulation into the forelimb motor cortex. It is important to note that our focus was primarily on the mechanism of recovery and was not aimed at testing a potential treatment, so we chose a lesion model that will most likely provide us with uniform lesions for easier analysis. This makes translation to the clinic difficult however, since most SCI patients suffer traumatic injuries of different magnitudes and at different spinal segments. Furthermore, cuts to the spinal cord that specifically sever the CST are very rare. Similarly, our choice of using cannulation for drug delivery aimed to increase the specificity of our treatment to our area of interest, which is the forelimb motor cortex, especially given the various and ubiquitous functions of PKA in the cortex.

A variety of PKA antagonists are available to study effects of PKA inhibition, including the compounds KT 5720 and H89. Our choice of using Rp-cAMPS was based on reports that this compound is the most specific to PKA with the least cross reactivity to other proteins from the AGC family (reviewed in Murray, 2008). Rp-cAMPS is a competitive antagonist of PKA, competing with cAMP for the same binding sites on PKA. At a drug dosage of 40nmol/injection, this compound is reported to be effective at inhibiting PKA activity when injected directly into rat cortices over short time periods of hours to days (Punch et al., 1997). Little is known about the stability of the drug in solution over a period of weeks, but our laboratory has previously observed treatment induced effects

using the drug infused through cannulation. We followed similar time courses and methods in the current study. To detected PKA inhibition, we probed for nuclear pPKA levels using western blot because PKA activity is increased when phosphorylated at T-197 (Steichen et al., 2010), and PKA activation results in increased diffusion of its catalytic subunits into the nucleus (Gervasi et al., 2007; Harootunian et al., 1993).

Lastly, we used 10 rats per group to assess recovery after SCI, which gave us sufficient statistical power for data analysis based on previous recommendations for the power required in behavioral research (Cohen, 1992). Our rats were young female adults, which allowed us to use task paradigms from, and compare results with previous studies performed in our laboratory. Between lesion and the start of recovery training, rats were allowed 1 week of rest due to previous findings that initiating training immediately after injury worsens behavioral outcomes after training (Krajacic et al., 2009). Behavioral recovery was measured using grasping performance and CST collateral sprouting, both of which were used previously in our laboratory. Our analysis does not differentiate between compensatory methods of grasping such as scooping pellets and true recovery of grasping. However, increased grasping success has been reported to be associated with increased CST sprouting, irrespective of compensation or true recovery (Girgis et al., 2007), so the same outcome measure was used in the current study. We also assigned rats to groups based on baseline grasping performance to ensure both groups had comparative grasping successes. The advantage of matching by grasping performance is that it eliminates the possible confound of different performance levels between groups prior to training, which is important because grasping success is one of the primary outcome measures of our study. The downside is that it may introduce biases in factors that were not examined, but may also impact grasping behavior. Given that grasping matching and random assignment both have advantages and disadvantages, we chose matching, which best suited our needs for the current study.

*e. Conclusions*

Several lines of evidence suggests that PKA activation by the second messenger cAMP may be important for training induced neurite sprouting and recovery after SCI. Foremost, increased PKA activation may convert the spinal cord to a more developmental like environment, with increased growth factor signaling and negation of the growth inhibitory effects of MAG. Increased PKA activation may also be involved in the degradation of Nogo A, and may attenuate inflammation and expression of the pro-apoptotic factor TNF. Given this prior evidence, the current study aimed to examine whether activation of the cAMP-PKA signaling pathway is necessary for neurite sprouting and training induced recovery after SCI. To do so, we inhibited PKA activation and tested the effects this had on the subsequent grasping training administered to rats with SCI.

Hypothesis: We hypothesized that inhibiting PKA will reduce training benefits, including inhibition of neurite sprouting, as well as exacerbate inflammation and lesion size.

## 2. Methods

*a. Examining the Effects of PKA Inhibition on Training Induced Recovery after SCI*

The main experiment examined the relationship between PKA activity and training after SCI. Rats received Rp treatment starting immediately after a DLQ lesion, and single pellet grasping training one week postlesion. Rp was administered for the duration of post-injury training. Functional recovery was examined using the SPG and horizontal ladder tasks. At the end of the experiment, rat spinal cords were dissected to examine collateral sprouting in the CST rostral to the injury. We also examined microglia levels (via IBA1 density and quantity of expression) and cortical lesion sizes to quantify the effect of treatment on inflammation and tissue damage around the drug delivery site. Figure 2 indicates the timeline from initial training to perfusion for this experiment.

Animal Housing. Adult female Lewis rats (n=10/group for main grasping experiment, n=2/group for western blot analysis, Charles River, Canada) weighing 180-200g at the beginning of the experiment were group housed 5 to a cage and kept on 12h:12h light/dark cycles. In experiments requiring grasping training, rats were food restricted each evening to 8g/rat to motivate performance of the SPG task. No target weight reduction level was set for the experiment, but animal weights were monitored twice a week during training and daily for the week post-surgery to check for steady weight gain (i.e. no fluctuations greater than 5% body weight in a single day and/or consistent weight loss). All experimental procedures were approved by the University of Alberta Animal Care and Use Health Sciences Committee and complied with the guidelines of the Canadian Council for Animal Care.

Groups. The majority of rats were divided into two groups (n=10/group) receiving DLQ lesions at level C4 in the spinal cord, and pump implantation delivering either Rp-cAMPS (Rp), or saline into M1 using cannulation. Prior to surgery, rats were assigned to groups based on grasping success using their pre-injury performance to ensure comparable average grasping success. To ensure comparable

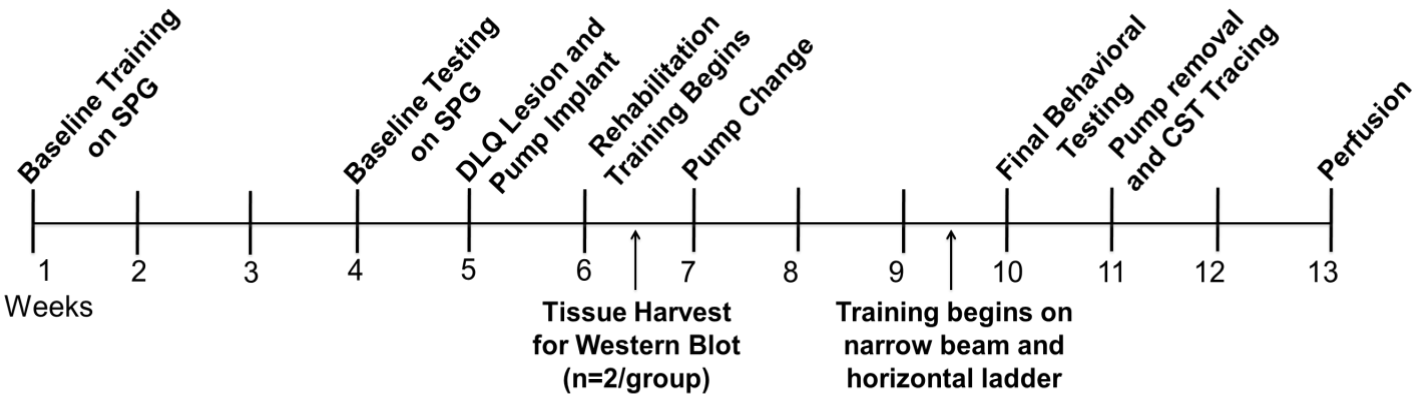


**Figure 2. Timeline of Experiment.**

attempt rates as well, rats had to perform at least 20 grasping attempts in a 10 minutes period during baseline testing to be included for post-lesion training. Rats that failed this criteria were included in the additional group described below for western blot analysis.

Two additional groups of rats (Western group; n=2/group) were used to quantify nuclear pPKA levels 10 days after lesion and treatment. The Western group rats were assigned to treatment prior to surgery, and received surgery at the same time as the other rats.

Spinal Cord Injury. All surgical procedures were performed between 8 AM and 3 PM during the day. The order of rats receiving surgery was staggered between treatment groups to prevent potential confounds involving fatigue of the surgeon. The injury consisted of a dorsolateral quadrant (DLQ) lesion at level C4 within the cervical enlargement. The lesion unilaterally severed the dorsal CST, as well as the majority of the lateral RST projections (Fig. 3). Rats were first anaesthetized using 5% isoflurane in air, and maintained in surgical plane using 2.5-3% isoflurane. Prior to placing onto the stereotaxic frame (Kopf Instruments, Germany), the skin around the upper back and scalp was shaved and then cleaned with 10% Chlorhexidine Digluconate (Sigma-Aldrich). An incision was made in the skin above the vertebrae C2-C4, and the overlying muscle was split. A partial laminectomy was performed over vertebrae C4. Subsequently, the lesion was made on the side of the rat's preferred paw by inserting a custom microblade to 1 mm depth into the cord at the midline and moved laterally. The overlying muscles and skin were sutured before minipump implantation.

Pump Preparation and Implantation. Osmotic minipumps (Model 2002, Alzet) and brain infusion kits (Kit 2, Alzet) were prepared the day before implantation. Briefly, the PKA inhibitor Rp-cAMPS (Rp, Tocris) dissolved in saline to 3.33 mM were syringe filtered (PVDF Membranes, Millipore) into 1.5 mL Eppendorf tubes. The filtered solution was transferred into pumps in sterile vacuum hoods, using dull-ended needles supplied by the manufacturer. Prepared pumps were kept in injectable saline at 37 $^{o}$C

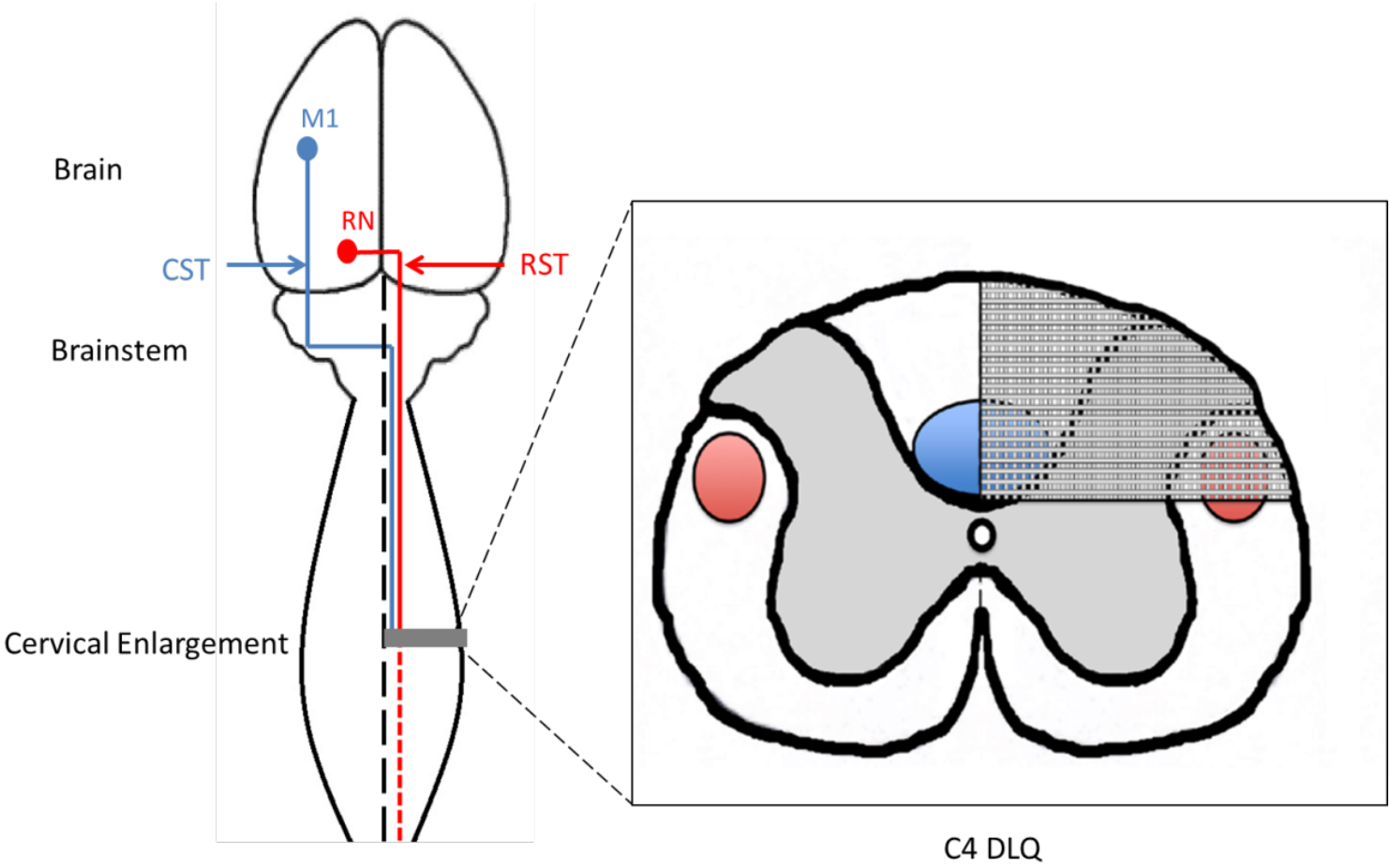


**Figure 3. The Lesion Model. Left**: dorsal view of the CST and RST that projects from the motor cortex (**M1, blue**) and red nucleus (**RN, red**) respectively. A DLQ lesion (**grey bar**) in the cervical enlargement unilaterally severed the major CST projection, as well as the majority of RST fibers (**red dashed line**). Midline is indicated by the black dashed line. **Right**: Cross sectional view of the DLQ lesion. The dorsal CST projection is indicated by the area shaded blue. The RST is indicated by the red circle. The lesion is represented by the grey grid.

overnight following the manufacturer's instructions. Injectable saline vehicle pumps were prepared the same way.

The same day, infusion cannulae were trimmed to target an insertion depth of 1.5 mm. Kits were attached to silicone tubing and left overnight at room temperature. Prior to implantation, tubing was rinsed first with 90% alcohol and then injectable saline, and cannulae were also tested for patency.

During pump implantation, the skin overlying the rat's skull is first cleaned with 10% Chlorhexidine Digluconate, then the skull is exposed with an incision. Throughout our experiments, we targeted the forelimb motor cortex by drilling a hole into the skull at coordinates 1.5 mm anterior and 1.5 mm lateral to bregma on the side contralateral to the injury (Fig. 4). After filling the tubing with vehicle or Rp solution, the rim of the kit is covered with an adhesive (Loctite; Cedarlane, Canada), and the cannula is inserted into the cortex through the hole. The tubing is attached to a pump, and the pump is then inserted subcutaneously between the shoulder blades. The skin overlying the skull is subsequently sutured.

Pump Change. Used pumps were taken out and replaced with fresh pumps every two weeks. Rats were anaesthetized using isoflurane for the procedure, and old pumps were removed through a skin incision made over the pump. Fresh pumps prepared the previous evening were inserted and attached to the tubing. Wounds were closed using surgical staples.

Post-operation Care. Rats were given the analgesic Buprenorphine (0.05 mg/kg; Temgesic) and 3 mL injectable saline S.C. immediately after each surgery. They were checked daily following pump implantations for signs of infections, as well as for major swellings around the pump and infusion kit that might cause discomfort.

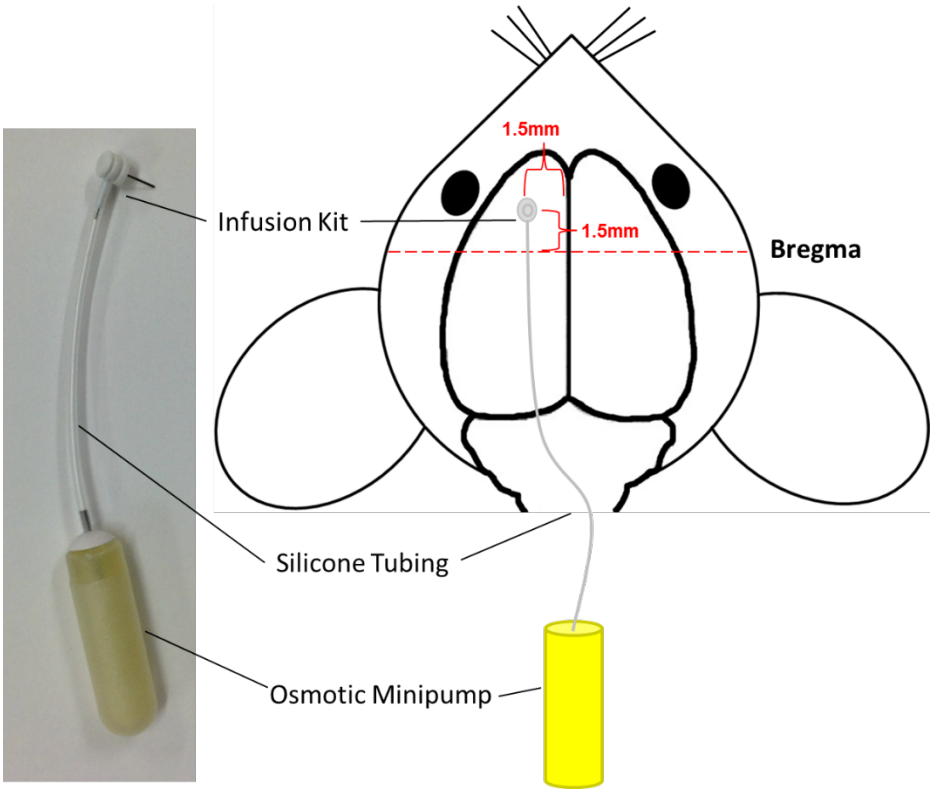


**Figure 4. Minipumps and Infusion Kit.** Left: Picture of a minipump attached to the infusion kit (with cannula) using silicone tubing. Right: Minipumps were implanted subcutaneously into the animal's back. The infusion cannula was inserted into the forelimb motor cortex at the indicated coordinates. Dashed red line indicates bregma.

Single Pellet Grasping. To successfully complete the SPG task, rats were required to reach through a narrow slit at the front of a Plexiglas chamber for sugar pellets (45 mg banana flavored; Research Diets) placed on the adjacent shelf (Fig. 5a). After each attempt, rats were required to go to the back of the chamber before a new pellet is presented on the shelf. The number of successful grasps and total number of pellets presented were counted. At the end of each session, the number of successes divided by total attempts is used to calculate grasping success.

Rats were familiarized with the SPG task for 4 weeks prior to surgeries and the start of rehabilitative training. This baseline training consisted of 10 minutes sessions of grasping, five times a week. To be included in the postlesion training, rats were required to perform at least 20 grasping attempts during this 10 minutes period. The grasping success during the last 3 days of training was used as baseline performance for each rat. Paw preference was also recorded during baseline training (Fig. 5b).

Rehabilitative training began one week following surgery. The post-injury training consisted of 15 minutes of grasping per day, five days a week for four weeks. Performance during final testing at the end of the training period was used to calculate each rat's postlesion grasping success. SPG protocols were performed in accordance with the methods stated in Krajacic et al. (2009).

Horizontal Ladder Task. For experiments using the horizontal ladder task, rats were placed on a platform joined by a ladder with unevenly spaced rungs to their home cage. Each animal was required to cross the ladder three times per testing session (Fig. 6a). Rung spacing was changed between testing days to prevent pattern learning. On each testing day, continuous ladder crossings for each rat was video recorded and used for later analysis. A mirror placed opposite the ladder was used to evaluate the paw opposite the camera.

Video analysis of performance on the horizontal ladder task was done using the software VirtualDub (GNU General Public License). Only the middle length of the ladder was used for analysis

(a) (b)

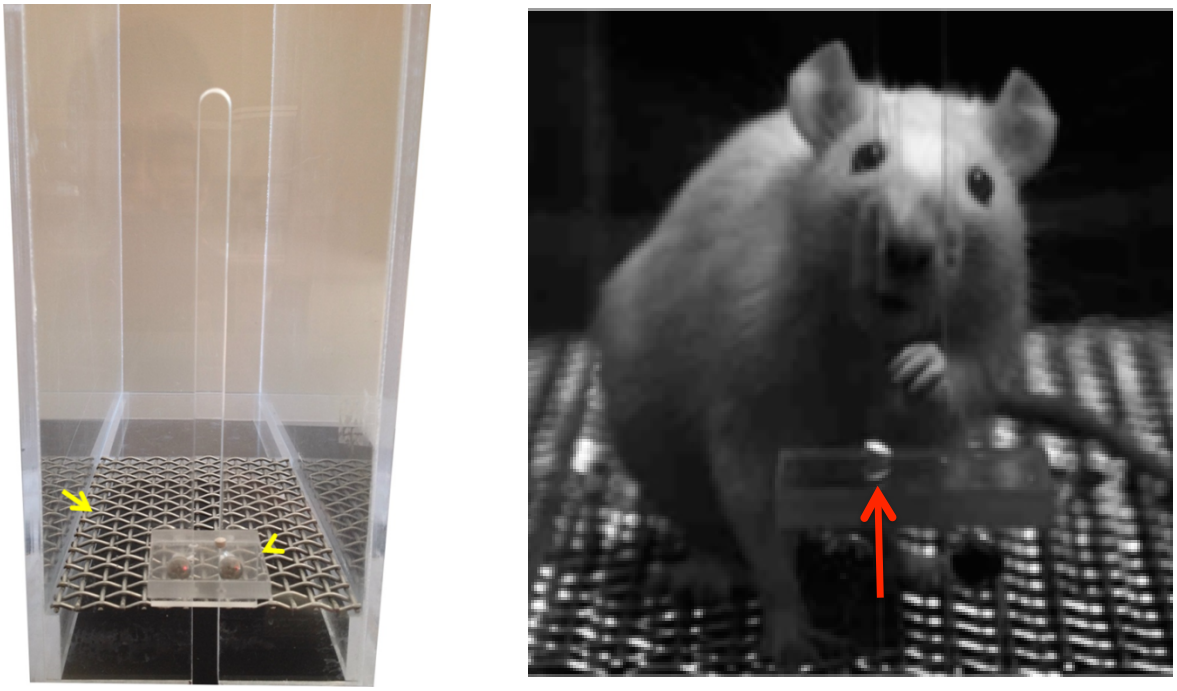

**Figure 5. The Single Pellet Grasping Task.** (**a**) Rats were trained on the single pellet grasping task using the plexiglas box. A pellet was placed on the platform for grasping (**yellow arrowhead**). If the pellet was dropped within the box, it fell through the wire-grid floor and became unreachable (**yellow arrow**). (**b**). Example of a rat performing the single pellet grasping task. **Red arrow** indicates the pellet was placed on the opposite side of the rat's preferred paw.

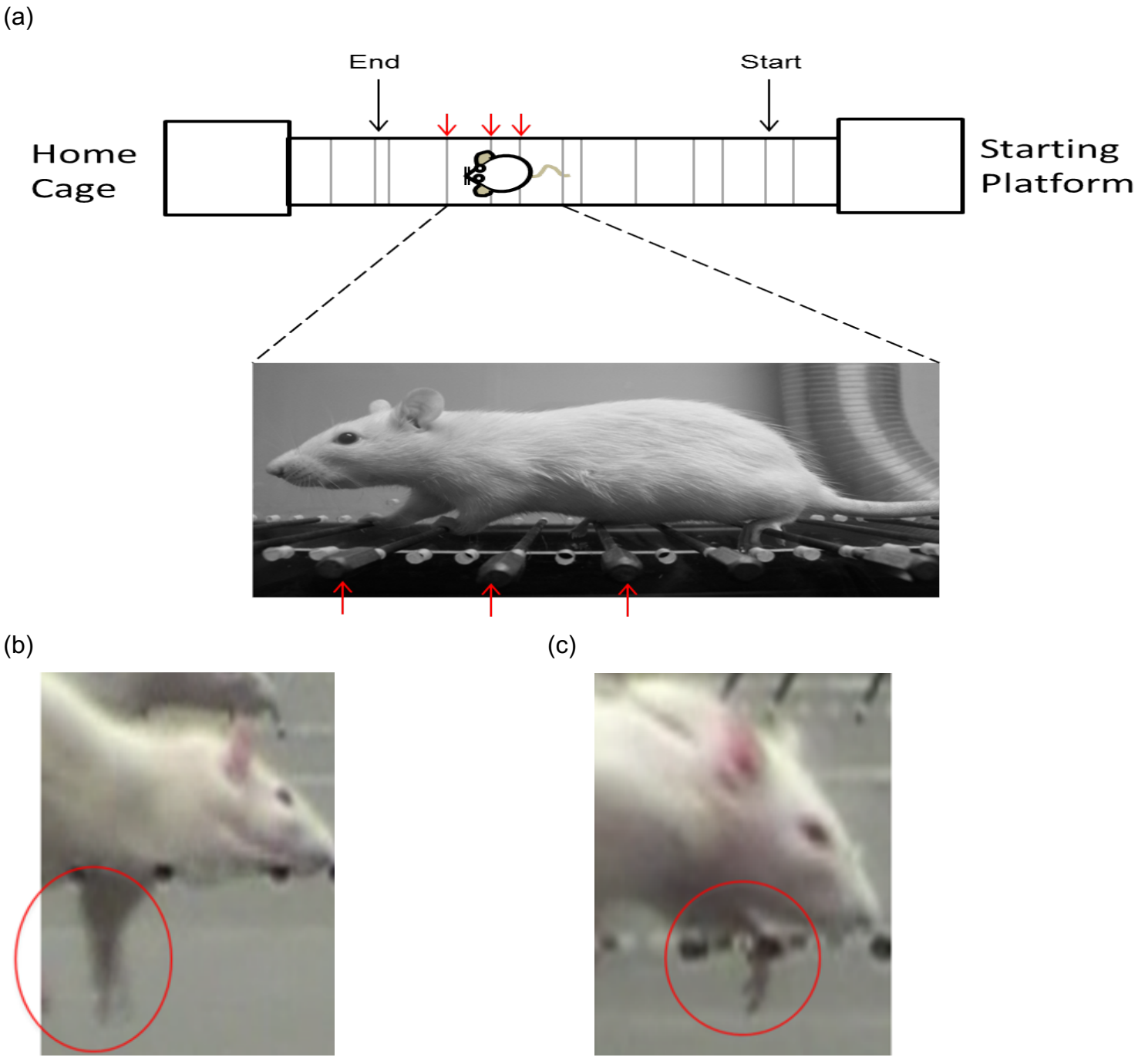


**Figure 6. The Horizontal Ladder Task.** (**a**) Rats were placed on the **starting platform** and encouraged to cross a horizontal ladder with unevenly spaced rungs (**red arrows**) to reach their **home cage**. The number of step cycles, paw slips, and compensatory movements were assessed using video over the distance indicated by **Start** and **End**. (**b**&**c**) Examples of paw slip (b) and compensation (c) made during a ladder crossing (**red circle**). Compensation was defined as using wrist contact instead of digit grasping of the rung.

to exclude the first and last step cycles. The analysis consisted of counting the number of step cycles, compensations, and paws slips for each paw per crossing. For statistical comparisons, the number of slips and compensatory movements (Fig. 6b, c) for each preferred and nonpreferred paw were expressed as a percent of the total number of steps taken by that paw. Horizontal Ladder protocols were performed in accordance with Krajacic et al. (2009).

CST Tracing. After final behavioral testing, rats were placed under 2.5-3% isoflurane anaesthetic, and the anterograde tracer Biotinylated Dextran Amine (BDA, 10%; Microprobes, USA) was injected into the contralesional forelimb motor cortex to visualize the CST. Following the procedures given in Krajacic et al. (2009), a 5 mm x 5 mm window was created in the skull over the contralesional forelimb motor cortex. A Hamilton syringe (Reno, USA) filled with BDA was inserted into the cortex to a depth of 1.5 mm and 1 µL of BDA was slowly injected over two minutes. The needle was left to sit for an additional 1 minute to prevent backflow before retraction. This procedure was then repeated at 2 additional sites in the area. Following tracing, the overlying skin was sutured, and post-op care given as described above.

Perfusion and Dissection. Ten days post-tracing, rats were euthanized with an overdose of pentobarbital (Euthanyl; Biomeda-MTC, Canada) and transcardially perfused using a solution of 0.9% saline with heparin followed by 4% paraformaldehyde containing 5% sucrose. Both the brain and the spinal cords were dissected and post-fixed overnight in 4% paraformaldehyde with 5% sucrose. Following fixation, brains and cords were cryoprotected in 30% sucrose for 3 days. The brain was divided into cortex and brainstem, and the spinal cord into C1 and C2-C6 sections for freezing. The freezing procedure consisted of covering tissue sections in tissue-tek (Sakura Finetek USA) and slowly submerging in methylbutane at -40$^{o}$ C. Frozen tissues were sectioned at 25 µm.

Spinal Cord Lesion Size Analysis. Horizontal C2-C6 sections were used to quantify the maximal lesion extent (Krajacic et al., 2009). Under phase contrast, and starting with the dorsal-most section, the lesion extent of each section was transposed onto a cross-sectional representation of the cord at level C4 (Fig. 7). Sections were analyzed every 100 μm until no more tissue damage were seen. Major landmarks such as changes in the size of the grey matter, the presence of the CST (visualized using 3,3'-Diaminobenzidine staining; DAB; Vector Kit SK-4100), and the central canal were used to determine the approximate dorsal-ventral location of each section. In addition, the sizes of the grey matter dorsal horns were used to adjust for any tilt in the plane of the section. After analysis, maximal lesion areas were expressed as a percentage of the total cross-sectional area for statistical comparison. All spinal lesion sizes were quantified by the experimenter under blind conditions.

Collateral Quantification. BDA staining was visualized in spinal sections by incubating successively with Avidin/Biotin Conjugate (ABC; Vector), and DAB following the manufacturer's instructions. Briefly, tissue was dehydrated by baking at 37$^{o}$C for 2 hours, then rehydrated successively in 2x TBS and 1x 0.5% TBS-Tx washes. Prepared ABC solutions were applied to each slide and incubated in a humid chamber for 60 minutes. Slides were then washed and reacted with DAB solutions. DAB reactions were halted by quenching in a distilled water bath. Slides were then dehydrated serially in increasing concentrations of alcohol before coverslipping with Permount (Fisher Scientific, Canada).

DAB reacted C1 sections were used to count total CST fibers traced in the dorsal CST projection (Fig. 8a; Vavrek et al., 2006). The averages of three sections were used as the quantity of total traced fibers. C2-C6 horizontal sections containing the CST were used to count collateral sprouting extending into the grey matter (Fig. 8b). Fiber counting started with the first section containing traced CST, and included every section 100 μm apart until no more CST was seen. Counting was performed at 40x on a Leica light microscope. The number of sprouting counted on horizontal sections was recorded at 1 mm intervals, starting from the edge of the lesion to at least 1

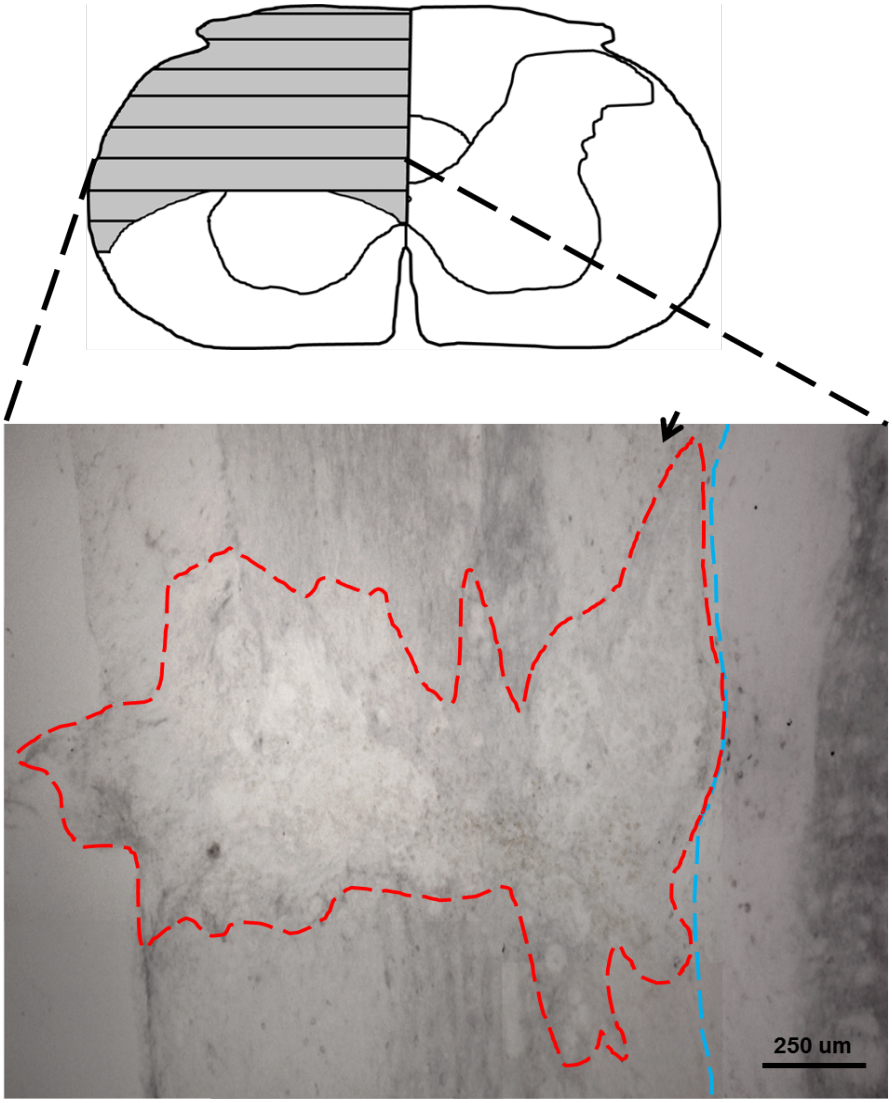


**Figure 7. Spinal Cord Lesion Size Analysis. Top**: Representative figure of a lesion transposed onto a cross-sectional diagram (**grey**). **Bottom**: Maximal lesion areas were determined using DAB stained C2-C6 horizontal sections viewed under phase contrast. The lesion area from each section (**red dotted lines**) was transposed onto the cross-sectional diagram as a horizontal line. **Black arrow** indicates the lack of traced fibers in the dorsal funiculus. **Blue dashed line** indicates the midline.

(a)

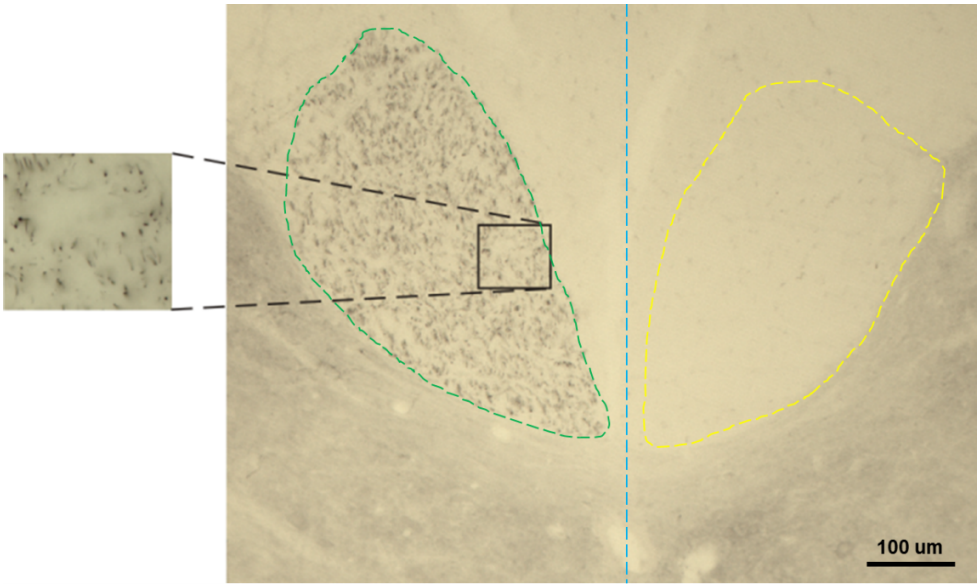


(b)

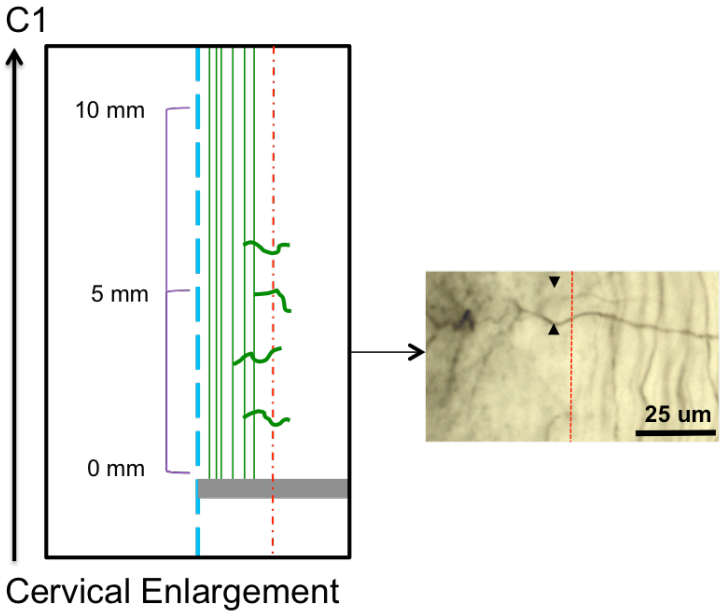


**Figure 8. CST Collateral Analysis.** (**a**) C1 cross section depicting traced CST fibers visualized with DAB in the right dorsal funiculus (**green dashed line**). Note the lack of DAB staining in the untraced funiculus (**yellow dashed line**). **Inset** depicts the magnification at which traced fibers were counted. (**b**) **Left**: Collateral fibers extending across the white/grey boundary (**red dashed line**) into the grey matter. **Green lines** indicate traced CST fibers. **Grey bar** indicates the lesion. At least 10 mm of tissue rostal to the lesion was analyzed for each section (**Purple Bracket**). **Right**: Example of collaterals (**arrowheads**) extending into the grey matter. **Blue dashed line** indicates midline.

cm rostral. We analyzed differences in the total number of traced fibers between groups, expressed as a percentage of total fibers traced per millimeter. All fiber counts were performed by the experimenter under blind conditions.

Microglia Quantification. Cortical sections 25 µm thick was used to quantify microglia levels around the site of cannulation by the experimenter blind to treatment. Activated microglia was visualized by incubating tissue sections with antibody targeting IBA1 (1:200; Wako), then reacted with the fluorescent Alexa Fluor 488 conjugated secondary antibody (anti-Alexa Fluor 488, 1:500; Molecular Probes, USA) before dehydration and coverslipping with permount. Fluorescent IBA1 expressing cells were visualized using a Leica fluorescent microscope and images were taken for analysis. Three sections from each animal were used for IBA1 densitometry measurements. The sections were taken from the rostral end of the lesion, the epicenter of the lesion, and the caudal end of the lesion (Fig. 9a). Pictures of these sections taken at 20x magnification were made into collages, thresholded in ImageJ, and 5 x 0.5 $mm^2$ regions that extend medial-laterally around the lesion cavity were drawn in layer V (Fig. 9b). Densitometry measurements were taken of 25% of the tissue area in each region, to avoid irregularities such as cavities in the tissue. The measured densities in layer V were then normalized to IBA1 densities in the striatum.

To examine whether there were changes in the number of microglia in response to treatment, we further counted IBA1 positive cells surrounding the lesion epicenter using stereology. Counting was performed at 20x magnification, in two 0.5 $mm^2$ regions adjacent to the lesion site (Fig. 9c). Densitometry methods were modeled on the methods described in Weishaupt et al. (2013).

Brain Lesion Size Analysis. The glial scarring resulting from cannulation and drug infusion was assessed under blind conditions by the experimenter on 25 µm thick cortical sections. Sections were incubated with primary antibody against GFAP (1:1000; Abcam) overnight, and then reacted with

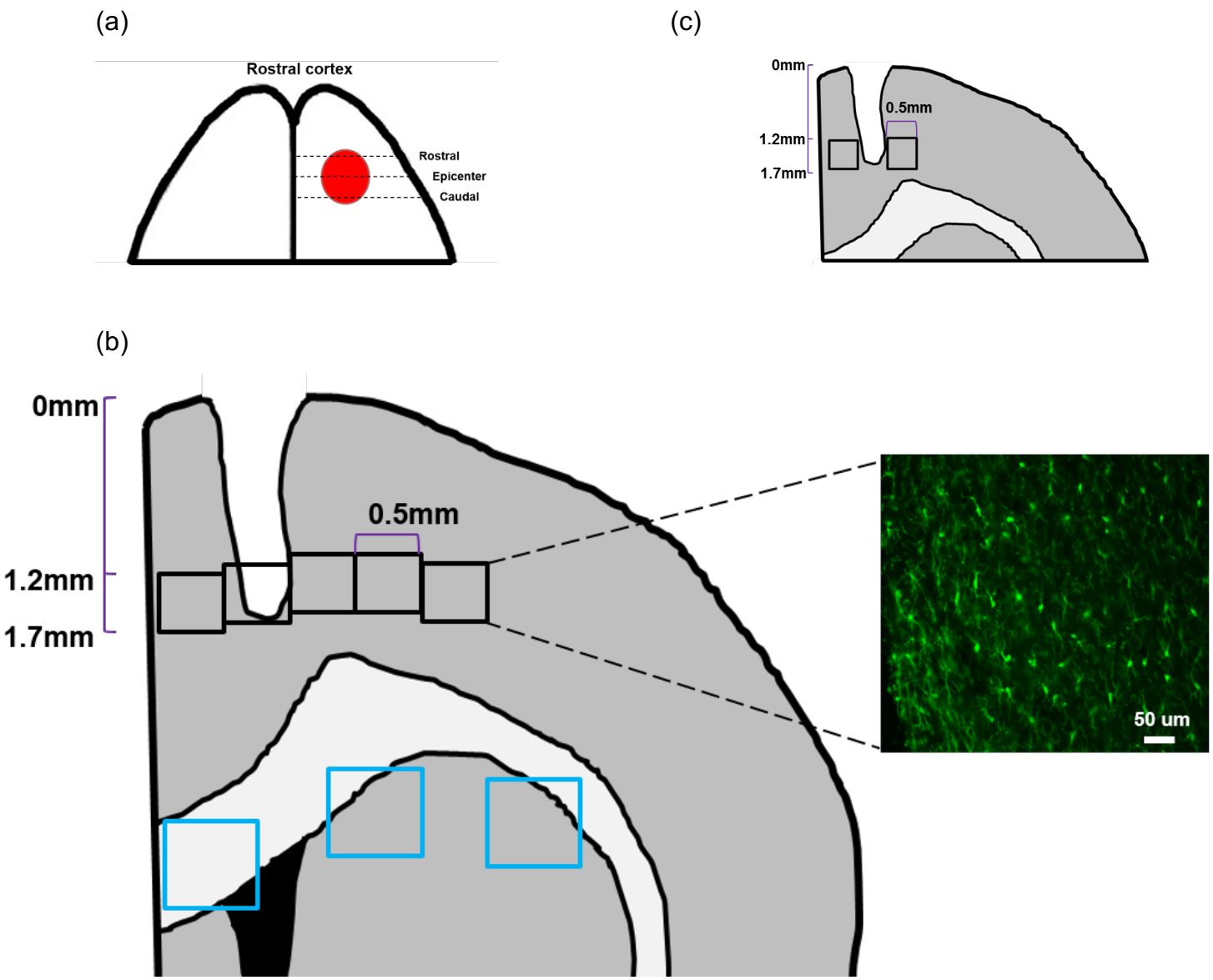


**Figure 9. IBA1 Quantification.** (**a**) IBA1 density was quantified at the rostral, epicenter, and the caudal end of the cortical lesions (**dashed lines**). **Red circle** represents the lesion. (**b**) Five 0.5 $mm^2$ windows were drawn from -0.5 mm to 1.5 mm medial-laterally to the lesion site in cortical layer V (**black boxes**). Three additional windows were drawn in the white matter and striatum of the same section (**blue boxes**) for normalization. (**c**) Using the sections containing the lesion epicenter, 0.5 $mm^2$ windows were drawn to the left and right of the lesion (**black boxes**). Total IBA1 expressing cells were counted at 20x magnification in these boxes.

Alexa fluor 488 conjugated secondary antibodies (1:500) and visualized using a fluorescent microscope. Images of the section with the greatest cavity and scar areas were taken under 5x magnification. We used three measurements to assess scarring. These included total cavity plus scar area, cavity area only, and scar thickness. Measurements were performed on collages of the lesion area using ImageJ (Fig. 10).

Tissue Harvesting. Rats from each group (blind to the experimenter) were decapitated without anaesthetic using Decapicones (Braintree Scientific Inc.), and an area of tissue approximately 5 mm in length was extracted and flash frozen in liquid nitrogen (Hurd & Fouad, Unpublished). Tissues were individually homogenized using a dounce homogenizer in freshly prepared sucrose buffer with protease and phosphatase inhibitors (10 mM HEPEs, pH7.6; 250 mM sucrose; 10 mM KCl; 1.5 mM $MgCl_2$; 1 mM EDTA & EGTA each; 2 µM aprotinin; 4 µM pepstatin; 20 µg/mL leupeptin; 1 mM PMSF; 1% v/v Phosphatase Inhibitor Cocktails 2 & 3; Sigma-Aldrich). Homogenates were then fractionated by centrifuging at 800g to precipitate the cell nuclei. The nuclear fraction was further lysed in a buffer containing 1% Triton X-100 (Sigma-Aldrich) to extract nuclear contents. The supernatant was collected as the cytosolic fraction after centrifugation.

Western Blot. Total protein concentration in each lysate was determined using the Bicinchoninic Acid (BCA; Life Technologies, Inc.) protein assay, and 10-20 µg of total protein was taken from the nuclear and cytosolic fraction of each animal to prepare loading samples (following procedures from Krajacic et al., 2009). After combining with 4x Sample Buffer and 10x Sample Reducing Agent (Novex), samples were boiled at $80^{o}$ C for 10 min in a hot water bath, and loaded onto Novex Minigels (Novex). Protein bands were separated at 200V, and transferred onto nitrocellulose membranes. Membranes were then washed in TBS with 0.5% Tween 20 (Sigma-Aldrich), blocked using Membrane Blocking Solution (Novex), and probed consecutively for PKA phosphorylated at threonine

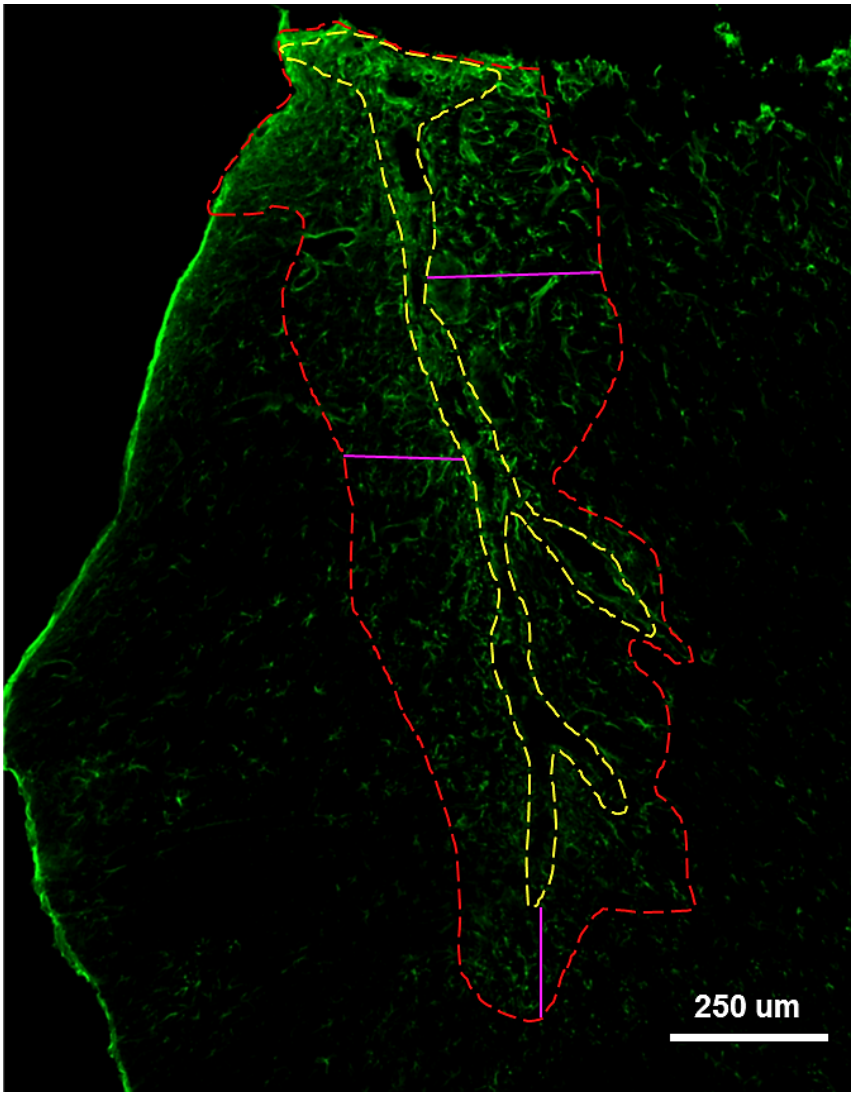


**Figure 10. Analysis of Glial Scarring with GFAP.** Total scarring and cavity area (**red dashed line**), cavity area (**yellow dashed line**), and average scar thickness **(purple lines)** were quantified for each animal at the lesion epicenter.

197 (rabbit anti-phospho PKA T-197, 1:2000; Cell Signal), total PKA catalytic subunits (rabbit anti-PKA Ca/b/y, 1:2000; Santa Cruz), Histone H3 (rabbit anti-histone H3, 1:5000; Cell Signal), and B-actin (rabbit anti-actin, 1:5000; Cell Signal). Membranes were incubated with horseradish peroxidase conjugated goat anti-rabbit secondary antibodies (1:2000; Cell Signal), followed by band visualization with ECL (Life Technologies) and exposure to X-ray films (Kodak; Fig. 11). Following each protein probe, membranes were stripped with Membrane Stripping Solution (Novex) and reblocked for the next antibody incubation. Developed X-ray films of bands were scanned onto a computer, and the band densities quantified using ImageJ (ImageJ, NIH).

Statistical Analysis. Student's t-tests, one-way ANOVA with Tukey's corrections for multiple comparisons, Pearson's correlation coefficients, and repeated measures two-way ANOVA with Bonferroni corrections for multiple comparisons for analyzing differences between groups were performed using Graphpad Prism v6.0 (Graphpad Software Inc, USA). All data were checked for normality (Shapiro-Wilk normality test) and equal variance (Bartlett's test). Any data failing normality test was analyzed with Mann-Whitney U-test correcting for non-gaussian distribution. Data are presented as means ± SEM, asterisks indicate significance: *P≤0.05.

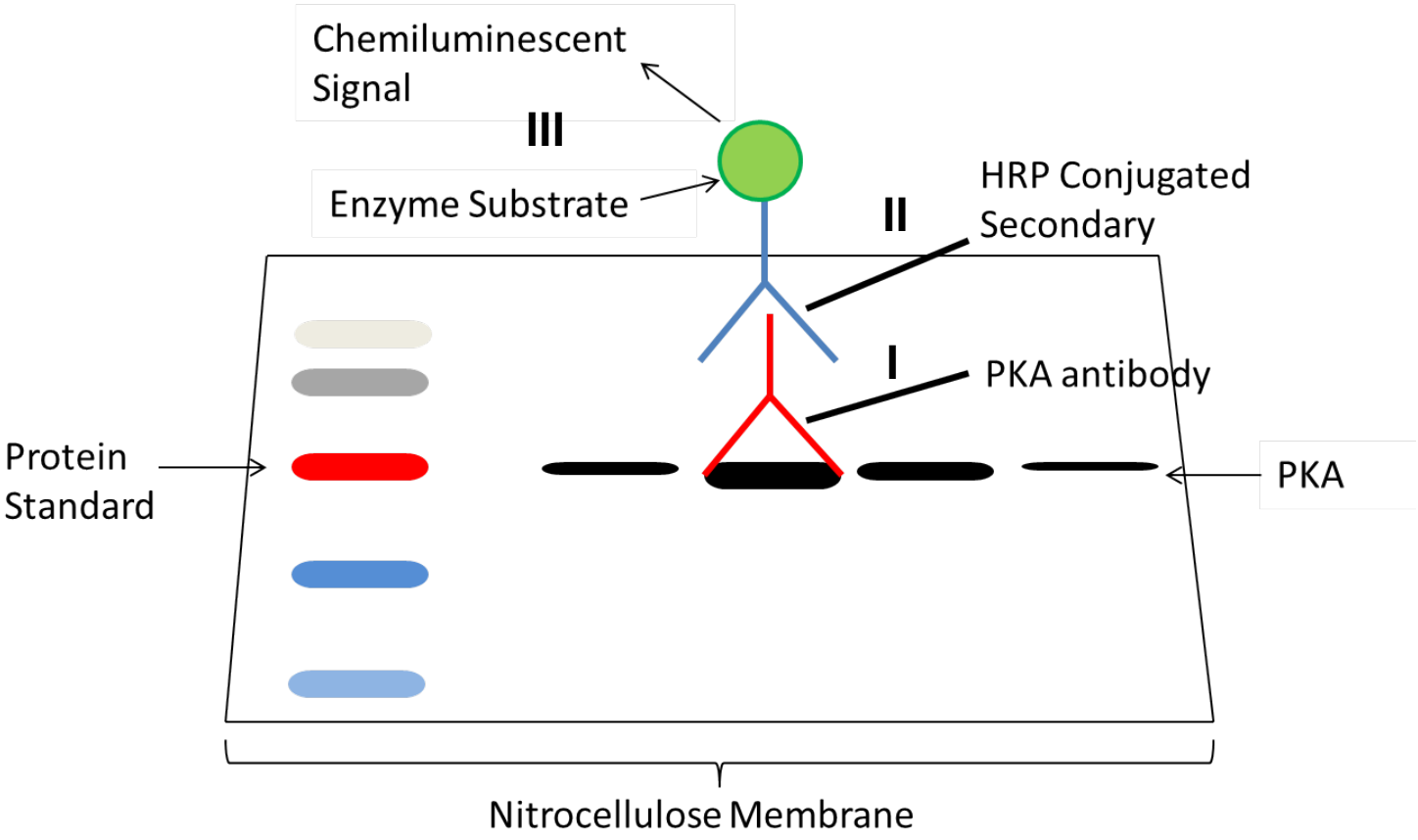


**Figure 11. Western Blotting.** Diagram of the western blot membrane and protein bands used to quantify proteins. The amount of protein (e.g. PKA) is quantified by incubating the membrane with a primary antibody (**I**) followed by the HRP-conjugated secondary antibody (**II**). The HRP is then reacted with a substrate to give off chemiluminescent signals (**III**). The intensity of the signal after exposure to x-ray films correlates with relative protein quantity (**indicated by bands of different thickness**). The **colored bands** on the left represents the protein standards used to estimate the molecular weight of a protein.

*b. Pilot Experiment Examining PKA Detection using Western Blot*

We additionally evaluated whether western blot can detect changes in pPKA levels following several pharmacological treatments, including after treatment with PKA agonists such as rolipram (Sigma-Aldrich) and Sp-cAMPS (Tocris), and in intact, untreated animals. Drugs were delivered into the forelimb motor cortex using cannula and minipumps for one week.

Groups. Rats were randomly assigned into five groups (n=2/group) receiving either: the selective PKA inhibitor Rp-cAMPS (40 nmol/day); the PKA activator Sp-cAMPS (40 nmol/day); the PDE4 inhibitor rolipram (10 nmol/day); vehicle only; or no treatment. Animal handling, pump implantation and post-op care was performed as described previously

Tissue Harvest. One week following pump implantation, cortical tissue around the cannulation site was extracted for western blotting as described previously. Pump implantation and Western Blot analysis were performed by the experimenter under blind conditions.

## 3. Results

*a. Rp Promotes Training Induced Recovery and CST Sprouting after SCI*

*Rp Treatment Promoted Functional Recovery*.

The main aim of the experiment was to test whether PKA activation is necessary for training induced recovery after SCI. Our hypothesis was that PKA inhibition would decrease the effects of training induced grasping recovery, so that rats given Rp would perform worse than saline treated rats. We first compared attempt rates between groups, and repeated measures two-way ANOVA indicated there was no significant effect of treatment over the training period (Treatment P=0.38; interaction of Time x Treatment P=0.99; Fig. 12a). Repeated measures two-way ANOVA analysis of grasping performance over time indicated that Rp treatment did not result in significantly different grasping successes compared saline (Treatment P=0.31; interaction of Time x Treatment P=0.41; Fig. 12b), even though Rp rats appeared to have higher grasping means over the course of the postlesion training period. When we compared grasping successes at final testing using Student's t-test however, the Rp group demonstrated significantly higher grasping success rates than the saline group on the SPG task (Rp: 40.3 ± 5.4%, saline: 23.6 ± 5.7%, P=0.046; (Fig. 12c). This was consistent with results from a previous experiment in our lab, where we also found higher grasping success in rats given Rp compared to saline treatment (Fig. 12d). We also observed significant effects of time on both attempts (P<0.0001) and grasping success (P=0.03) over the training period.

Several studies have previously indicated that training on one task may affect performance on untrained motor tasks after SCI (Girgis et al., 2007; Krajacic et al., 2010; Starkey et al., 2011). We wanted to assess whether the demonstrated recovery was task specific, and whether untrained tasks such as horizontal ladder crossings were affected by the combination treatment. Video analysis of the number of paw slips (Fig. 13a) made during ladder crossing suggested no difference between groups (preferred paw: saline=3.1 ± 1.3%, Rp=0.5 ± 0.5%, Student's t-test: P=0.1; nonpreferred paw: saline=2.4 ± 1.6%, Rp=1.0 ± 0.7%, Student's t-test: P=0.45). Similarly, no difference was detected

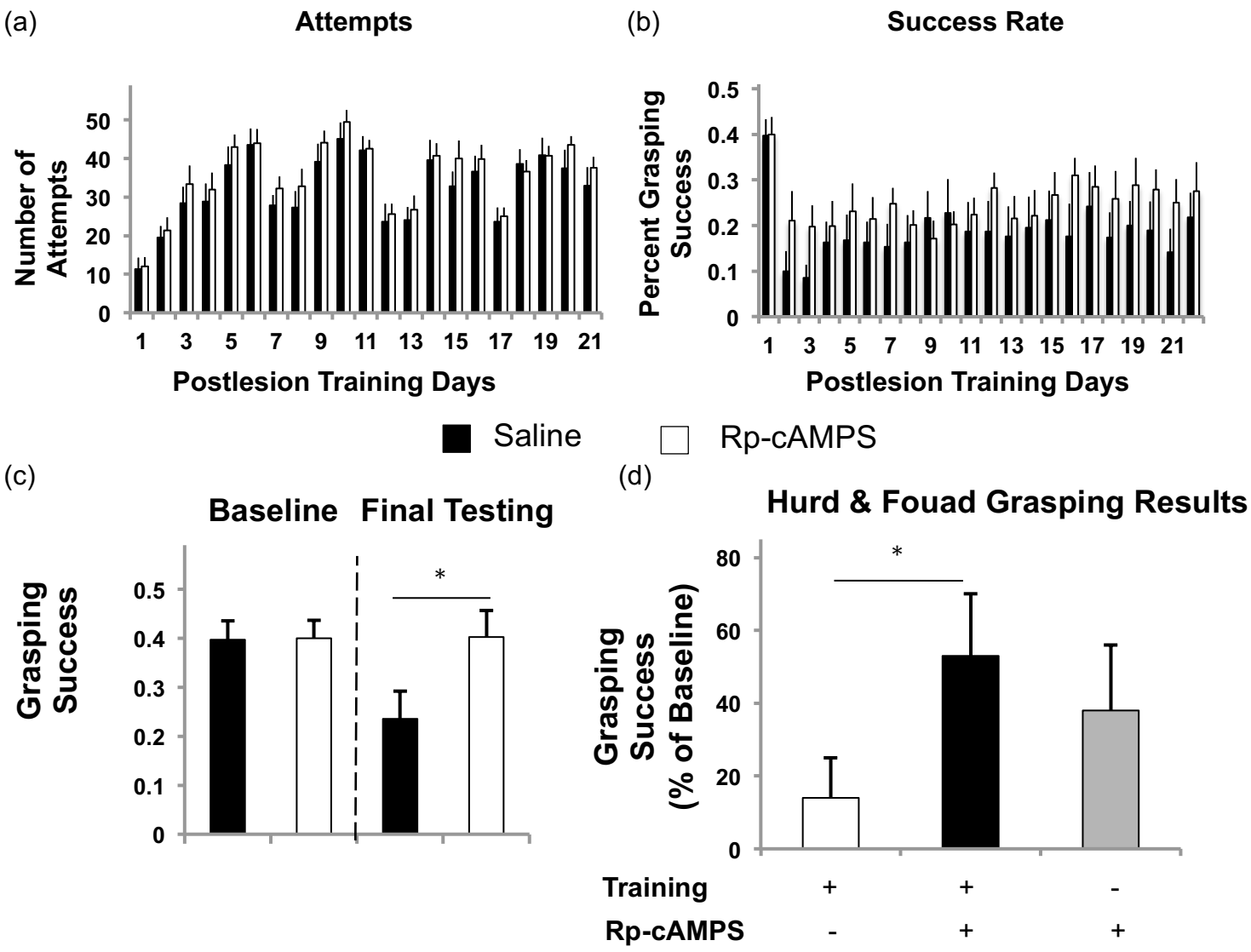


**Figure 12. Pre- and Post-Injury Grasping Performance.** (**a**) Quantifications post-injury attempt rates. The number of attempts between groups were not significantly different on any day over the postlesion training period (two-way ANOVA treatment P=0.38). (**b**) Postlesion grasping successes over the course of the training period. Rats in the Rp group had higher average grasping successes on most days over the course of training, but these differences were not significant on any day (two-way ANOVA treatment P=0.31). (**c**) Comparisons of Baseline and final testing grasping successes between groups. The groups had comparable average success rates at baseline, while Rp treated rats had significantly higher success rates compared to saline treated rats at final testing (P=0.046). (**d**) Grasping results from Fouad & Hurd (Unpublished). Rp treatment and training (black bar) resulted in significantly higher grasping successes compared to saline and training (white bar; P<0.05), while Rp treatment (grey bar) alone resulted in higher grasping successes compared to saline, although this was nonsignificant. n=10/group. Black bars represent saline and white bars represent Rp treatment for graphs **a**-**c**.

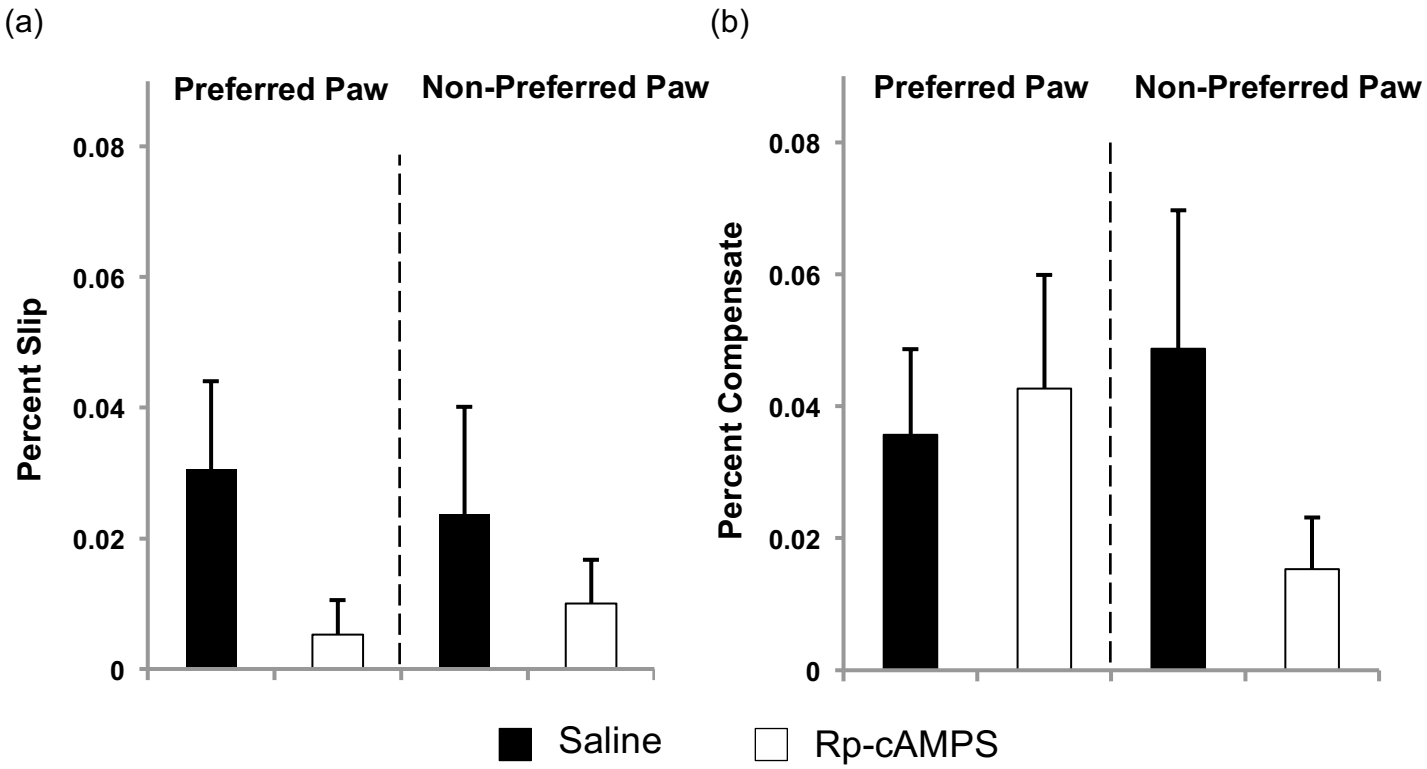


**Figure 13. Horizontal Ladder Results.** (**a**) Comparisons of the number of paw slips expressed as a percentage of total steps made by that paw. (**b**) Comparisons of the number of compensation movements expressed as a percentage of total steps. Dashed black line divides the performance of preferred and non-preferred paws in each graph. n=10/group.

between groups on the number of compensatory movements (Fig. 13b) made during crossing (preferred paw: saline=3.6 ± 1.3%, Rp=4.3 ± 1.7%, Student's t-test: P=0.75; nonpreferred paw: saline=4.9 ± 2.1%, Rp=1.5 ± 0.8%, Student's t-test: P=0.15).

*Effect of Recovery was not due to Differences in Lesion Sizes*. Before analyzing neuroanatomical changes, we quantified lesion sizes to examine whether they were comparable between groups. The averages of the maximal lesion area between groups were not significantly different (saline=22.3 ± 2.3%, Rp-cAMPS=26.7 ± 4.5%, Mann-whitney U test: P=0.86; Fig 14a), even though Rp rats had higher average lesion sizes. Furthermore, we observed no significant correlations between percent lesion areas and final grasping success (r=-0.089, P=0.71; Fig 14b).

*Rp Increased Collateral Sprouting into the Grey Matter*. Fibers extending into the grey matter from the damaged CST rostral to the injury are associated with better recovery after SCI. To examine whether the greater recovery demonstrated by rats given Rp was also associated with greater CST sprouting, we quantified the number of collaterals extending from the damaged CST into the grey matter rostral to the lesion. We began by counting the total number of traced fibers at C1, which was needed both for normalization of collateral sprouting, as well as to examine whether there was a difference in tracing between groups. Our analysis indicated no significant differences in the total number of traced fibers between groups (Rp=288.7 ± 81.0 fibers, saline=374.3 ± 39.2 fibers, Student's t- test: P=0.36; Fig 15a). Next we counted the number of collateral sprouting, and observed that the average number of collaterals extending into the grey matter after Rp treatment was 0.9 ± 0.2% fibers/mm, whereas for the saline group it was 0.5 ± 0.08% fibers/mm (Student's t- test: P=0.046; Fig 15b). We further correlated final grasping success to the number of collaterals, and observed no significant correlations between the two factors (r=0.06, P=0.82; Fig. 15c). Lastly we

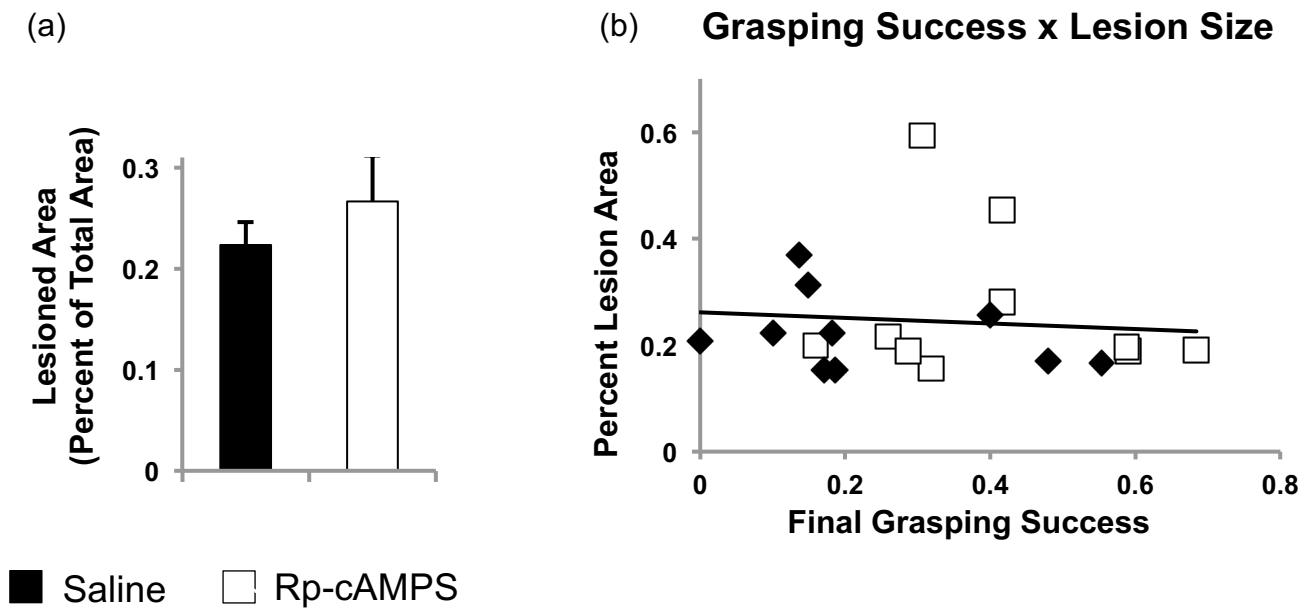


**Figure 14. Lesion Size Quantification.** (**a**) Comparison of the maximal lesion areas for each group. The maximal lesion area was expressed as a percentage of the total cross-sectional area. There were no significant differences between groups (P=0.86). (**b**) Correlation between lesion area and grasping success (black line). Pearson's correlation coefficient indicated that the two factors were not correlated (r=-0.089). Black diamonds indicates individual saline rats, white squares indicates individual Rp rats.

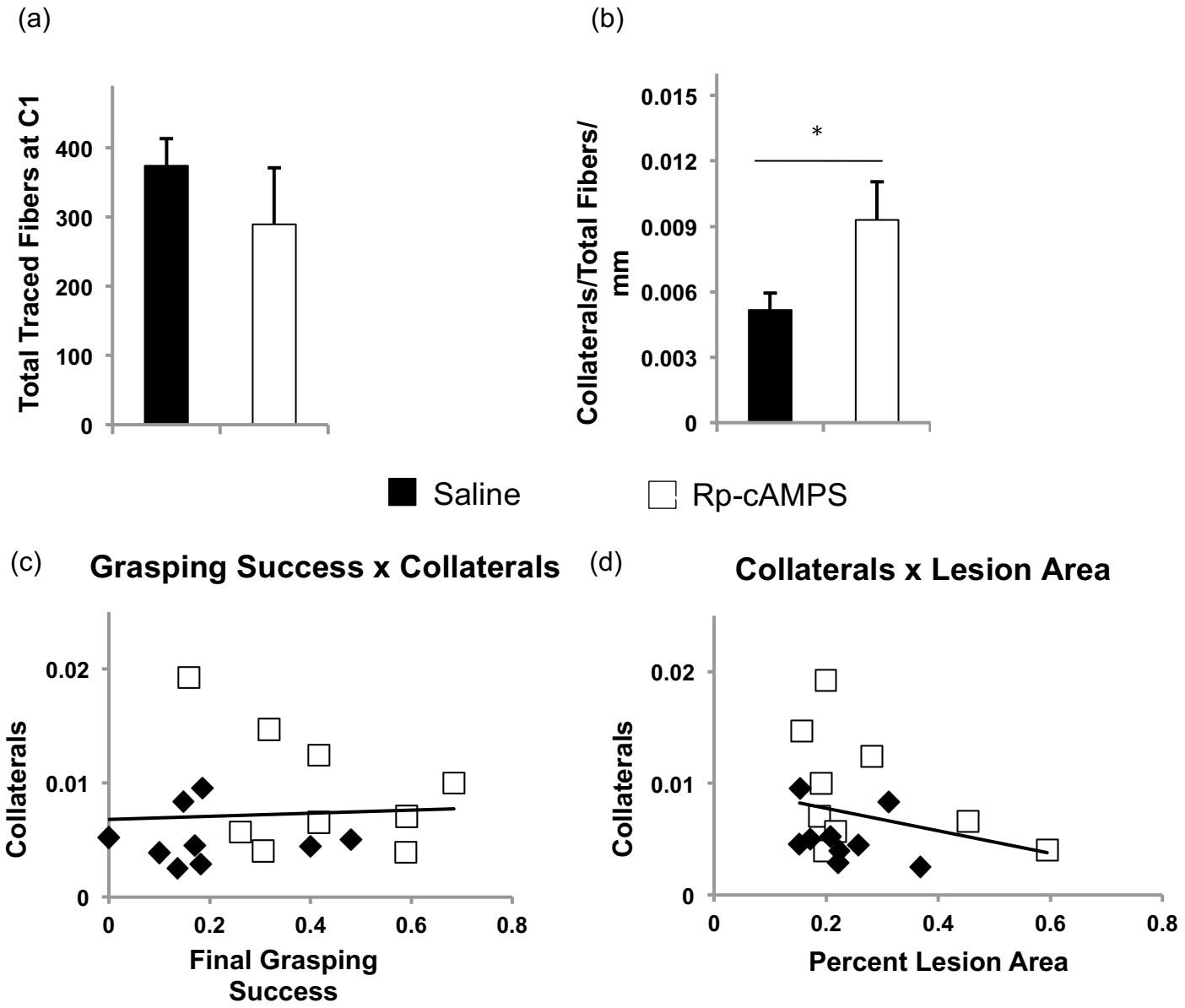


**Figure 15. Collaterals Quantification.** (**a**) Comparison of the total number of CST fibers counted at C1. Total traced fibers were not significantly different between groups (P=0.36) (**b**) Comparisons of the total number of collaterals extending into the grey matter between groups. The number of collaterals was expressed as a percentage of total fibers traced, and normalized to distance quantified (mm). Rp rats had a significantly higher number of collaterals than saline rats (P=0.046). (**c**) Correlating final grasping success to lesion area. Pearson's correlation coefficient indicated no significant correlations between the two factors (r=0.06, P=0.82) (**d**) Correlating the number of collateral sproutings to lesion area. Pearson's correlation coefficient indicate no significant correlations between the two factors (r=-0.26, P=0.29). n=9/Group. Black line in **c** and **d** represent the correlation trendline. Black diamonds represent individual saline rats. White squares represent individual Rp rats.

examined correlations between collaterals and lesion size, where we again observed no significant correlations (r=-0.26, P=0.29; Fig 15d).

*Rp-cAMPS did not affect Cortical Microglia Quantity*. PKA activation has been linked to decreased microglia activation and decreased inflammation associated cell death (Woo et al., 2003; Atkins et al., 2007). Based on these findings, we hypothesized PKA inhibition also exacerbates inflammation, and may contribute to worsened recovery with Rp treatment. To examine this possibility, we quantified the levels of IBA1 expressing cells in cortical layer V of rats, focusing around the cannulation site. Due to the variability in the lesion size from animal to animal, we did not use tissue sections from fixed coordinates for analysis. Instead, we defined “rostral”, “epicenter” (or maximal lesion area), and “caudal” areas of the lesion, and chose sections within these approximate ranges. Furthermore, we divided each tissue section into five 0.5 mm regions, starting from the medial edge of the cortical section, and separately quantified IBA1 expression within each medial-lateral region. We observed no differences in IBA1 density between treatment groups at any medial-lateral distance in either the rostral, middle or caudal sections, although there were differences in IBA1 expression at different distances to the lesion in all three areas (Rostral: two-way ANOVA, interaction P=0.58, F=0.72, df=4; treatment P=0.17, F=1.95, df=1; distance P=0.005, F=0.005, df=4; Fig 16a. Epicenter: two-way ANOVA, interaction P=0.99, F=0.07, df=4; treatment P=0.55, F=0.37, df=1; distance P=0.001, F=10.14, df=4; Fig 16b. Caudal: two-way ANOVA, interaction P=0.69, F=0.56, df=4; treatment P=0.99, F=0.001, df=1; distance P=0.002, F=4.69, df=4. Fig. 16c). The significant effect of distance from lesion (two-way ANOVA, $P<0.001$) indicates that the highest density of microglia is found around the lesion area in both groups.

Differences in IBA1 density may not represent differences in microglia quantity. To confirm our observation that saline treatment resulted in increased inflammation in cortical layer V compared to Rp treatment, we further counted the number of IBA1 expressing cells. Counting was performed in

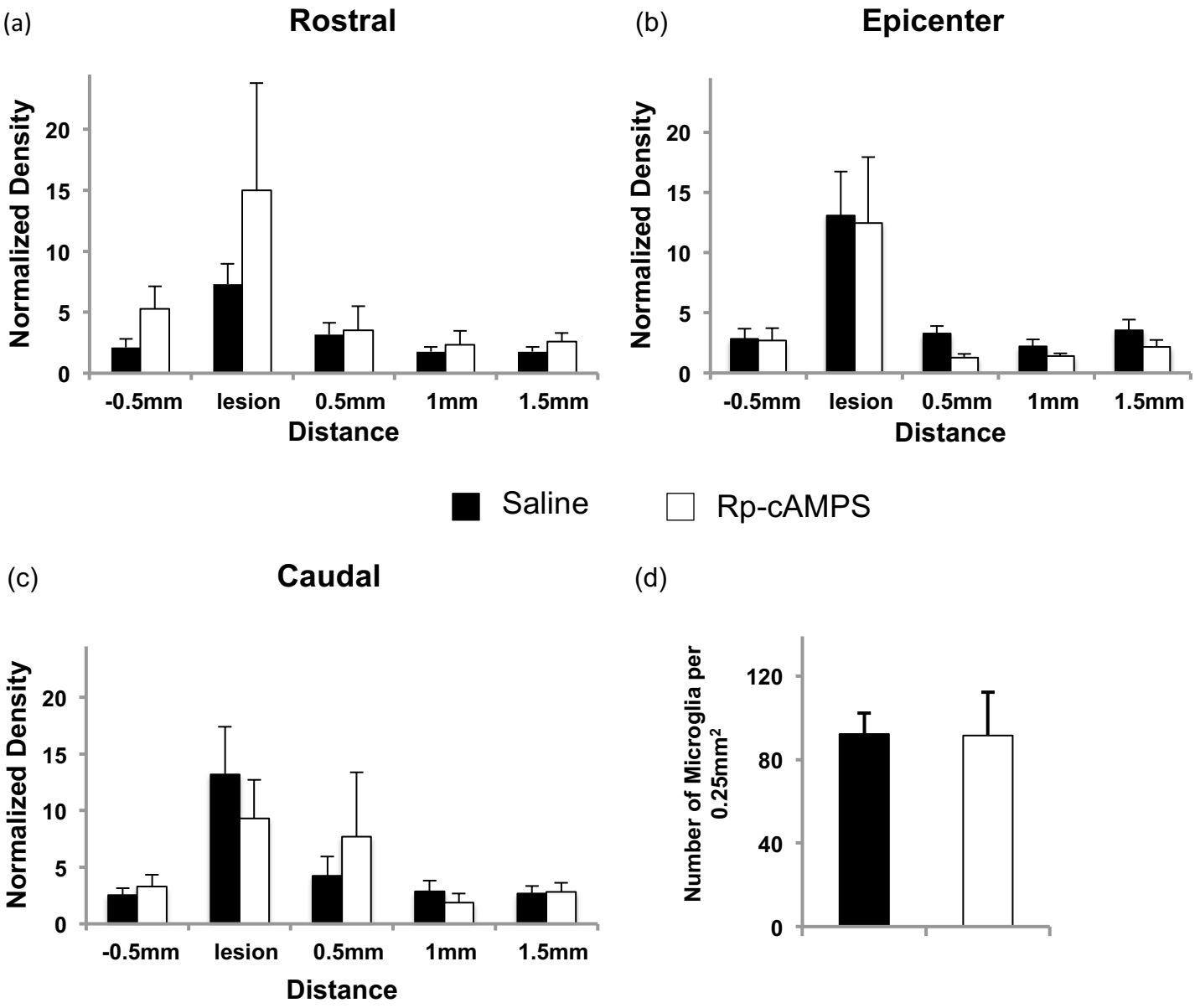


**Figure 16. IBA1 Densitometry and Stereology Results.** (**a**)-(**c**) IBA1 quantifications using densitometry at the rostral, epicenter, and caudal end of the cortical lesion. There were no significant treatment effects in the rostral, middle or caudal sections (two-way ANOVA treatment rostral P=0.17, epicenter P=0.55, caudal P=0.99). (**d**) Similarly, comparison of IBA1 expressing cell counts at the lesion epicenter did not yield any differences (P=0.97). Saline, n=9; Rp-cAMPS, n=8.

two 0.5 $mm^2$ boxes in the epicenter sections around the lesion site. Our results suggested no difference between groups in the number of IBA1 expressing cells at this site (saline=92.22 ± 10.09, Rp-cAMPS=91.50 ± 20.65, P=0.97; Fig. 16d).

*Rp did not affect Cortical Lesion Sizes*. Increased inflammation is associated with increased secondary tissue damage after CNS injuries (reviewed in Borgens & Liu-Snyder, 2012). We hypothesized that increased inflammation associated with PKA inhibition may lead to greater tissue cavities around the site of injection. Because increased tissue damage may also result in greater recruitment of reactive astrocytes to the injury site, we also hypothesized that rats with greater cavity will have thicker glial scars. To test these hypotheses, we measured the total lesion area (scar plus cavitation), cavitation, and scar thickness for each animal at the lesion epicenter. We found no significant differences between groups in total lesion area (saline=0.87±0.16 $mm^2$, Rp=0.81±0.17 $mm^2$, Student's t-test: P=0.80; Fig. 17a), cavitation area (saline=0.39±0.14 $mm^2$, Rp=0.27±0.12$mm^2$, Student's t-test: P=0.54; Fig. 17b), or average scar thickness (saline=0.13±0.03 $mm^2$, Rp=0.13±0.02 $mm^2$, Student's t-test: P=0.95; Fig. 17c). Thus, our results indicated that Rp treatment did not significantly alter lesion size or scar thickness at the cortical lesion site.

*PKA Quantification*. Lastly, we examined whether Rp treatment decreased nuclear pPKA levels in the rat motor cortex after SCI. Following 10 days of drug or vehicle treatment, we extracted rat cortical tissue around the cannulation site, and fractionated the lysed tissue to obtained the nuclear fraction. Using western blot to detect pPKA levels normalized to either total PKA catalytic subunits (PKAc) or the nuclear loading control Histone H3, we observed no consistent differences in pPKA band densities between treatment groups (Fig. 18).

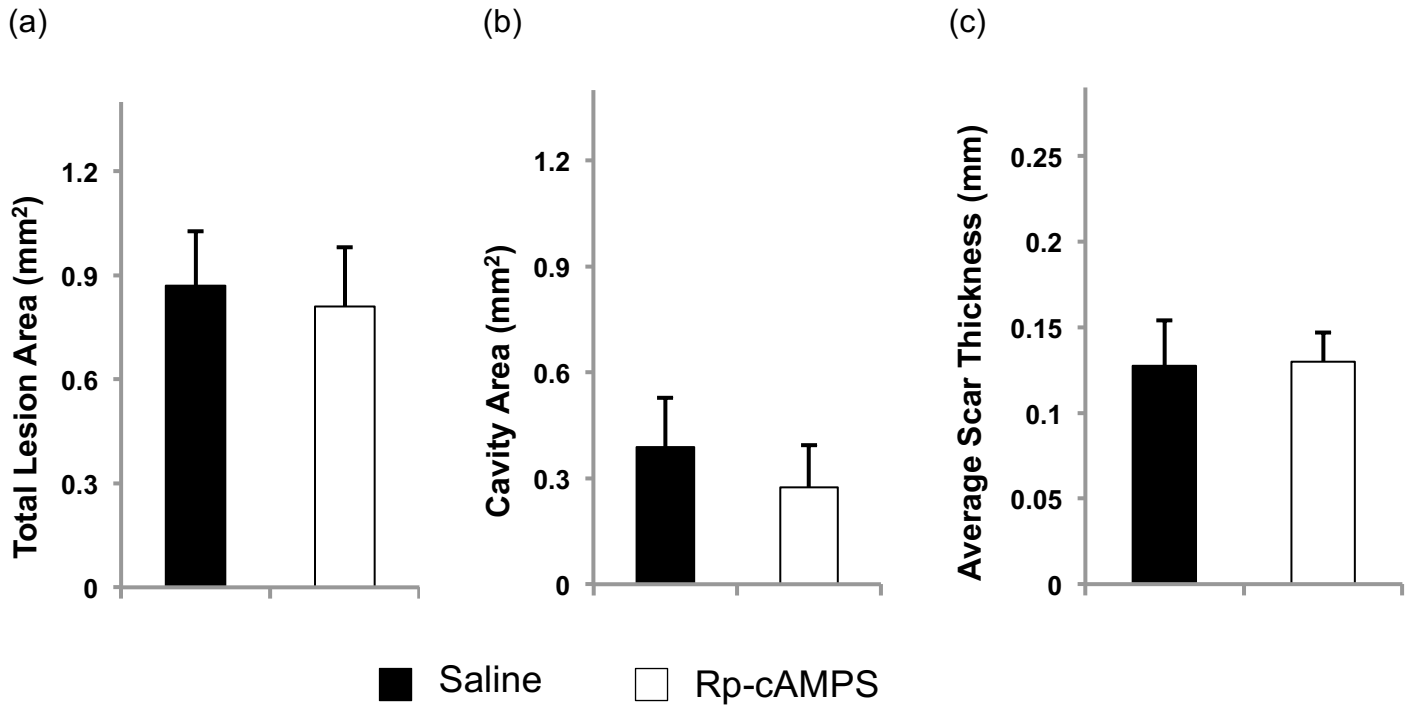


**Figure 17. Cortical Lesion Size Analysis.** Comparisons of (**a**) total lesion area (cavity plus scar), (**b**) cavity area, and (**c**) scar thickness between groups. No significant differences between groups were observed (total area P=0.80, cavitation area P=0.54, scar thickness P=0.95). Saline n=9; Rp-cAMPS n=8.

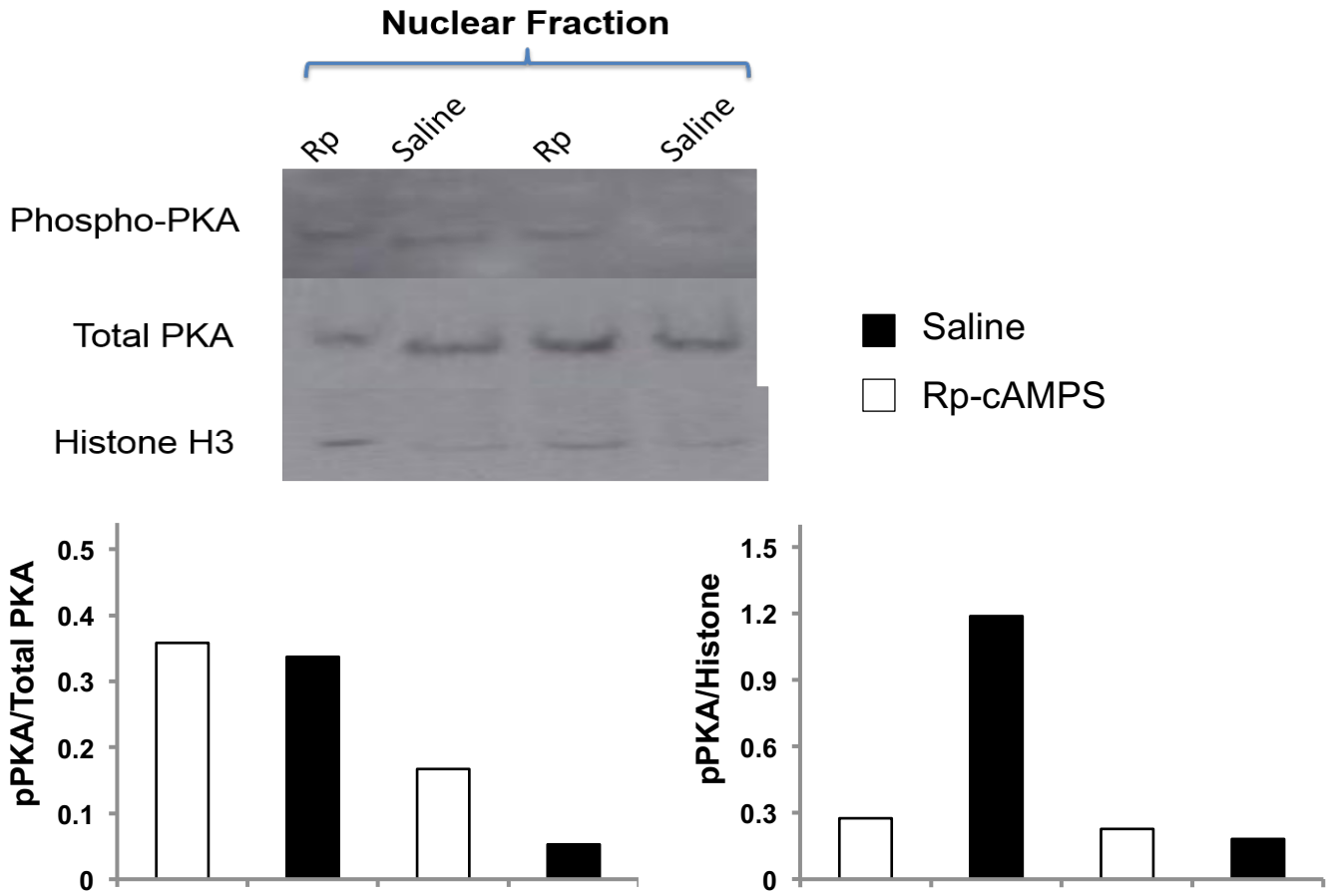


**Figure 18. PKA Quantifications. Top:** Bands of pPKA, total PKA, and the nuclear loading control Histone H3 obtained from western blots of rat cortical tissue after Rp or saline treatment. Each band represents 1 rat (n=2/treatment). **Bottom Left:** Quantifications of pPKA expressed as a fraction of total PKA.

*b. Quantifying pPKA Levels after Various Pharmacological Treatments*

*PKA Quantification*. The aim of this pilot experiment was to further assess whether changes in pPKA levels can be detected by western blotting, both before and after drug treatment in intact animals. We performed nuclear fractionation of drug treated cortical tissues and examined pPKA levels in this fraction after Rp, Sp, Rolipram or saline treatment. We only detected a decrease in pPKA band density, normalized to PKAc, in one of the rats given Rp treatment (Fig. 19a), and neither Sp or rolipram resulted in consistent increases in normalized nuclear pPKA levels after treatment compared to saline (Figure 19.a,b).

In a separate group of rats, we compared Rp and saline treatment to untreated rats to determine whether our treatment affected basal nuclear pPKA levels. Once again, Rp treatment did not consistently decrease nuclear pPKA levels compared to saline, when normalized to either total PKAc or the nuclear loading control Histone H3. Additionally, there were no differences in band density between treated and untreated rats (Fig. 19c).

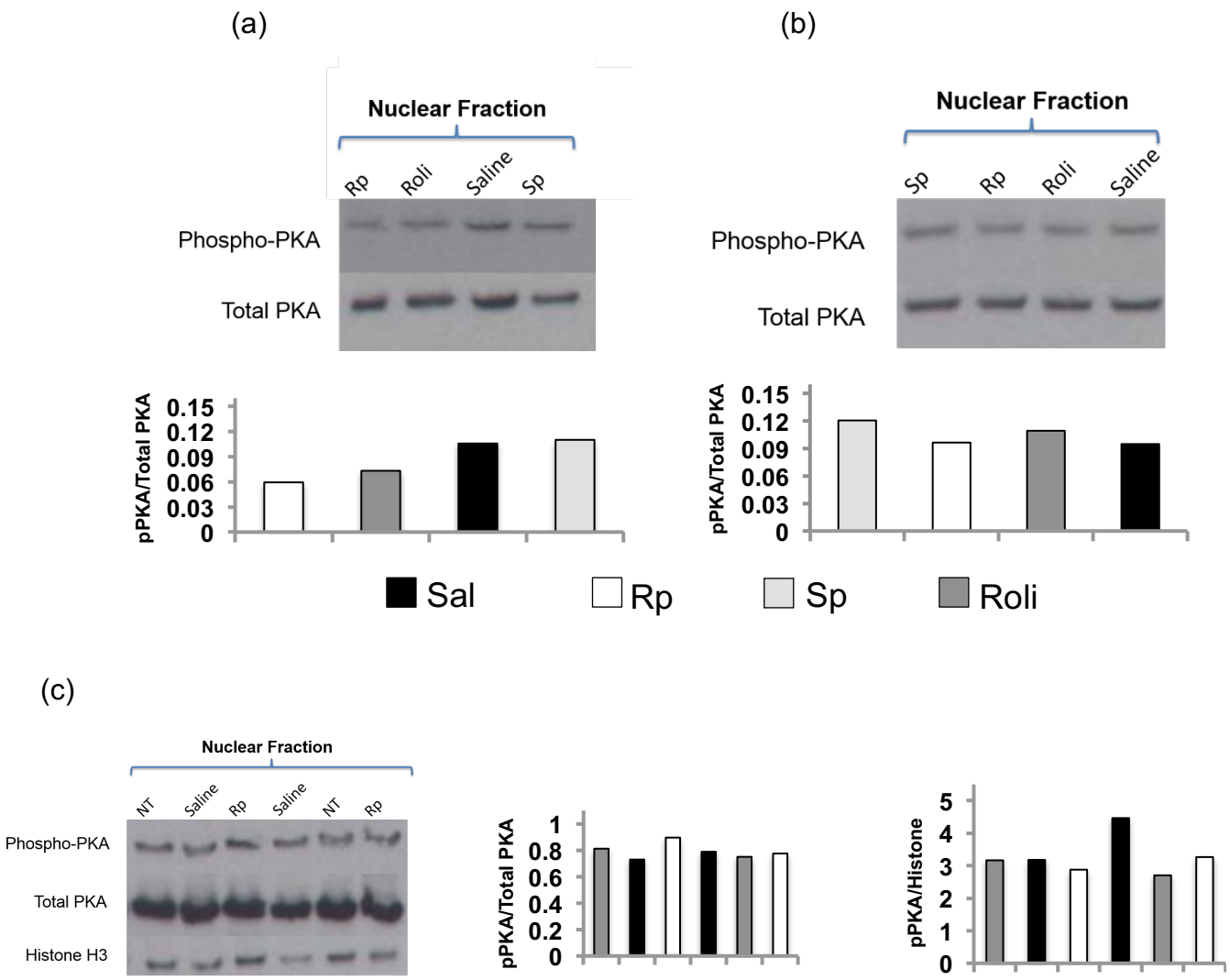


**Figure 19. PKA Quantifications of Pilot Experiment.** (**a & b**) **Top**: Bands of pPKA and total PKA obtained from the nuclear fraction of rat cortical tissues. Each band represents 1 rat (n=1/treatment). Each lane displays pPKA and total PKA levels for 4 rats. **Bottom**: Quantifications of pPKA densities in the nuclear fraction, expressed as a fraction total PKA density. (**c**) **Left:** Bands of pPKA, total PKA, and the nuclear loading control Histone H3 of untreated, Rp treated, or saline treated rats. Each band represents 1 rat (n=2/treatment). **Middle & Right:** Quantification of pPKA densities in the nuclear fraction, expressed as a fraction of total PKA (**Middle**) and Histone (**Right**). NT: no treatment; Sal: saline vehicle; Rp: Rp-cAMPS; Sp: Sp-cAMPS; Roli: Rolipram.

## 4. Discussion

*a. Behavioral and Histological Effects of Rp Treatment on Grasping Recovery*

Contrary to our original hypothesis, grasping training was not hindered by Rp-cAMPS treatment. But in line with the earlier Hurd & Fouad (unpublished) experiment, we observed increased grasping success in Rp treated rats compared to the saline group after SCI. Furthermore, we did not observe significant differences in attempt rates between groups. It was also interesting to observe that Rp rats had higher average grasping successes starting from day 1 compared to saline (Fig. 12b). The lack of an Rp only group in the current study makes it difficult to conclude whether we had a training effect. However data from Hurd & Fouad (unpublished; Fig. 12d) suggest that although rats given Rp had increased grasping successes without training, rats given Rp and training had even higher grasping successes, indicating that the observed effect was not due to Rp alone. Neuroanatomically, this difference in grasping performance may be a result of either greater neuroprotection after SCI or greater neurite sprouting in the Rp group.

To rule out neuroprotection, we examined possible differences in lesion sizes between groups. Our analysis involved quantifying the maximal lesion area at C4 in each group. We decided to use lesion area instead of volume because we were particularly concerned with the amount of CST and RST that was damaged. Damage to a tract such as the CST disrupts all connections below the point of injury, so we only needed to know what percentage of the tract was damaged on a cross section to gauge the severity of the lesion. Lesion volume may become an issue if the lesion destroys the ventral horn motoneurons, but this was not observed in the current study. Although there were no significant differences in lesion sizes between groups, we did observe a larger average lesion size in the Rp group compared to the saline group. We further determined that there was no correlation between grasping success and lesion size ($p=0.71$, Fig. 16b), suggesting that lesion sizes were not a contributing factor to the observed recovery after Rp treatment, and may instead indicate that grasping recovery in the Rp group was slightly underestimated in our results. Furthermore lesion

placement were likely similar between groups, because our analyses of CST sproutings terminated 1 cm rostral to the lesion, which also coincided with the end of the tissue sections.

To examine the effect of Rp treatment on neurite sprouting, we quantified the number of fibers extending from the injured CST into the grey matter in regions rostral to the injury. We observed that rats in the Rp group had a significantly higher number of collateral sprouting extending into the adjacent grey matter compared to rats receiving saline. One hypothesis for the beneficial effects of collateral sprouting is detour formation through contact with propriospinal interneurons (Vavrek et al., 2006), which may increase the activation of motoneurons and muscles involved in grasping, leading to grasping improvement. Despite this hypothesis, our correlation analysis between grasping and sprouting indicated no significant correlation between the two factors ($r=0.06$, $P=0.82$). However, it was difficult to conclude based solely on correlation that there was no association between treatment and sprouting, primarily due to the lack of untreated groups in the current study. But we also questioned whether it was useful to define a complex motor behavior such as grasping with only a single anatomical indicator. For example Hurd et al. (2013) reported that only rats with lesions approximating the DLQ range were able to demonstrate significant grasping improvements following training on SPG. Their initial meta-analysis correlating grasping improvements to lesion size in more than a hundred rats failed to suggest any correlation between the two factors. These results indicate a complex interplay between lesion size and training effects, and may suggest that other factors such as lesion sizes and individual attempt rates has to be controlled for to yield a conclusive correlation analysis between grasping success and collaterals. Consequently this would require a greater number of rats than used in the current study for statistical analysis to be meaningful.

Lastly, we were interested in whether grasping training with Rp affected performance on an untrained task. Performance of the horizontal ladder task also required forelimb grasping, and a previous study by Girgis et al. (2007) found that rats trained on grasping using SPG had worse performance on the untrained horizontal ladder task. The authors hypothesized that this effect was

due to the limited capacity of the injured CST to reorganize. With training, all remaining neuronal capacity is devoted to the ability to grasp, so even the performance of similar tasks are hindered. Originally we hypothesized that rats given Rp would perform worse than those given saline no matter the task, because PKA signaling is required for sprouting and reorganization to occur. Such a finding would further confirm the importance of PKA in sprouting and recovery after SCI. However, our results demonstrated no difference in horizontal ladder performance, despite grasping performance differences. It is unclear why this difference in training effect exists, but one explanation may be that rats in the Girgis et al., (2007) study underwent a more intense training regimen that utilized more of their remaining neuronal capacity than rats in the current study. Alternatively, our current result may reflect the late time point at which horizontal ladder assessment was performed in the present study. This is suggested by the minor error rates demonstrated by both treatment groups during testing. We may need to perform the horizontal ladder task at several time points during postlesion training, as well as at baseline testing in future experiments to determine whether our observed effect was an actual effect of treatments, or the result of testing at a single time point.

The major finding of the current study, that Rp-cAMPS treatment improved grasping success, contradicts the initial hypothesis we formulated, which was based on previous experiments such as MacDonald et al. (2007). Although this is surprising, it is certainly not uncommon due to the relative functional obscurity of cAMP's other downstream targets such as EPAC. Less than two decades ago, EPAC was still considered a novel cAMP effector (Rooij et al., 1999), and it was not until relatively recently that experiments began defining its role in neurite outgrowth (Murray et al., 2009; Woolfrey et al., 2009). As researchers learned more about the novel effector EPAC, their findings also suggested distinct roles for PKA and EPAC activation, and these roles some times opposed each other (Murray et al., 2009; Boomkamp et al., 2014). For example Murray et al. (2009) observed that, contrary to the simpler picture of neurite attraction mediated by increased cAMP-PKA signaling (Song et al., 1997), increased PKA activation may actually be a neurite repulsive signal, whereas EPAC activation

mediates neurite attraction. So while our current findings appear to contradict MacDonald et al. (2007), our study using a PKA specific inhibitor may be more nuanced than the former study, which used a general facilitator of all cAMP dependent activities.

*b. Identifying the Role of PKA in Training Induced Recovery*

The current experiment primarily depended on the ability to stably and chronically deliver drugs to animals, so we chose direct cortical infusion using osmotic minipumps. The use of minipumps for drug delivery has been used previously in our lab (Fouad et al., 2005; Hurd & Fouad, unpublished), and it offers two advantages for chronic drug delivery. The first is minimal stress to animals. Stress is an important factor for recovery after CNS traumas, and studies using rat stroke models indicate that post-lesion stress may increase lesion size as well as behavioral deficits after injury (Kirkland et al., 2008). This may occur through increased production of stress hormones, which is an aggrevator of inflammation during acute exposures, thus weakening the survivability of injured neurons after a neurotrauma (reviewed in Sorrells et al., 2009). Through the use of minipumps, we eliminated the additional stressor of daily drug injections to animals. The second advantage of using minipumps is the specificity of brain infusion kits in targeting a brain region. This is especially important because PKA is a ubiquitous protein in the CNS, and exerts a variety of effects upon activation. It was also critical for us to limit PKA inhibition to the cell bodies of CST neurons, as our hypothesis involved the inhibition of PKA dependent gene expression in the nucleus. Lastly, the inhibitor Rp-cAMPS used in this experiment does not readily cross the blood-brain barrier, so systemic injections were unfeasible. We achieved specificity by targeting the cannula to layer V of the forelimb motor cortex.

In light of the behavioral and histological findings, we attempted to establish that the observed effects were due to PKA inhibition via Rp-cAMPS. To detect changes in PKA activity in response to drug infusion, we probed for nuclear pPKA levels using western blot in samples of freshly harvested cortical tissues. This was based on previous studies indicating that activated PKA catalytic subunits eventually dissociates into the nucleus (Allen & Zhang, 2006; Gervasi et al., 2007). The additional lack of behavioral symptoms such as stress signs, seizures, or weight fluctuations in the majority of rats during Experiment III further supported this conclusion. However, we failed to detect a consistent decrease in nuclear pPKA levels in the Rp treatment group. This result was further confirmed in other

studies performed in our laboratory using striatum neuronal cultures treated with the same concentration of Rp. The cause of this inconsistency may be due to individual differences in the feedback mechanisms that maintains homeostatic activity in many biochemical pathways. Chronic Rp inhibition of PKA may have triggered increased production of cAMP differently in each rat, resulting in the inconsistent results seen in our western blots.

To address the possibility of a feedback mechanism, we gave rats a DLQ lesion prior to pump treatment. This was to reduce individual differences in baseline PKA activity between rats, which may aid in increasing the signal to noise ratio resulting from injury suppressed cAMP-PKA signaling activity in damaged neurons (Pearse et al., 2004; Krajacic et al., 2009). But once again we did not detect consistent decreases in nuclear pPKA levels after Rp treatment compared to saline. Our behavioral and histological results suggested that Rp treatment had an effect in the motor system, so we searched for alternative explanations for the lack of detectable changes in nuclear pPKA levels using western blot. Foremost, both Krajacic et al. (2009) and Pearse et al. (2004) suggested that activity in the cAMP signaling pathway are suppressed for at least two weeks following SCI and in the absence of treatment. So we may have detected a floor effect, where the activity in the cAMP pathway was still too low to result in detectable differences after Rp inhibition. Future experiments may need to quantify nuclear pPKA levels after longer treatment periods. Alternatively, western blotting may not be sensitive enough to detect changes in pPKA levels. Possible ways to compensate for the low sensitivity may be to increase sample sizes to decrease the effect of inter-animal variability for baseline PKA activity. As well increased sample sizes may average out the effect of inter-animal variability in the development of drug tolerance over time. Additionally, we may explore other techniques to detect Rp inhibition of PKA, such as using FRET (Fluorescence resonance energy transfer) and the PKA activity reporter AKAR3 to image PKA activity in different cellular compartments after treatment (Allen & Zhang, 2006).

*c. Possible role of PKA Modulated Inflammation on Recovery*

PKA inhibition may increase inflammation, increase lesion size and worsen recovery after Rp treatment. This was based on findings that PKA suppresses microglia activation by inhibiting TNF production (Yoshikawa et al., 1999; Pearse et al., 2004). Our densitometry data suggested that cortical damage increased the density of IBA1 expressing cells at the injury site, and Rp treatment decreased IBA1 density at the lesion epicenter. However, stereological analysis did not reflect a similar difference in the number of IBA1 expressing cells around the cannulation site. When we examined cortical glial scarring and cavity size, which may also be used as indicators of secondary damage, we again found no differences between treatment groups. It was tempting to conclude that the increased density of IBA1 expression in the saline group suggested greater inflammation in that group, despite the lack of differences in the number of microglia cells. However there is a paucity of studies examining an association between the levels of IBA1 expression and severity of inflammation. One study by Romero-Sandoval et al. (2008) reported an association between increased IBA1 densities with increased pain in rats, which may reflect increased inflammation. However the authors did not count the number of IBA1 expressing cells in addition to quantifying density, so it is difficult to rule out an increase in the number of microglia that underlies their correlation.

An explanation for the lack of observed effects on microglia levels and cavity size after Rp treatment may involve the delayed time point when we measured microglia levels. Previous studies indicated that microglia levels peak twice after injury. The first peak occurs one week after SCI and declines in the following days (Ito et al., 1998). This decline reverses over a longer time period, and microglia levels steadily increase to a second peak at three months post-injury (Beck et al., 2010). Our perfusion date at approximately two months post-injury fall near the peak of this upward slope, so our measure of total levels of activated microglia may not have been sensitive enough to detect a treatment difference. An alternative approach may require measuring subtypes of activated microglia.

Activated microglia are divided into the classically activated M1 subtype, which responds to stimulants such as TNF, and the alternatively activated M2 subtype (reviewed in David & Kroner, 2011). These two subtypes of microglia have different expressions of surface proteins, which have been used as distinguishing markers (Kigerl et al., 2009). Probing for these cell specific markers, we may quantify the ratio of M1 to M2 microglia, and determine whether there is a difference in this ratio between groups. Since PKA affects TNF expression, we may expect levels of subtype M1 to be higher in the Rp treated group, which will in turn suggest an effect of Rp on inflammation that was undetectable using only IBA1.

Although there is a negative association between inflammation resulting from PKA inhibition and recovery, we initially hypothesized that increased inflammation may underlie the cause of recovery after Rp treatment. This hypothesis was based on previous experiments suggesting that classically activated M1 microglia may be beneficial to neurite sprouting after injury (Rapalino et al., 1998; reviewed in Donnelly & Popovich, 2008). Because our IBA1 results did not deny this hypothesis, we may further examine inflammation by directly promoting the M1 phenotype in the cortex of rats and testing whether it has an effect on training mediated recovery after SCI. This may be achieved by injecting the microglia activating bacterial enzyme lipopolysaccharide (LPS) into the motor cortex.

*d. Future directions*

The major findings of this study are that Rp treatment in the cortex promotes behavioral recovery measured by grasping success and CST sprouting in rats after SCI. Future studies need to focus on establishing PKA inhibition, and linking it to recovery. As well further studies need to examine how recovery occurs with PKA inhibition. To address the first focus, we may use activity reporters to examine PKA inhibition, as described by Allen & Zhang (2006). In addition, we may examine targets downstream of PKA, such as the nuclear protein CREB, and measure CREB phosphorylation in response to Rp treatment. Previous studies reported, for example, that PKA inhibition in rodent hippocampal neurons led to a decrease in both the amount of CREB phosphorylated at serine 133 and CREB dependent transcription (Impey et al., 1998; Vitolo et al., 2002). We may also quantify PKA regulatory subunits after Rp treatment. PKA activity is regulated in part by the regulatory subunits of this tetrameric protein, and previous evidence suggested that prolonged PKA activation results in degradation of the regulatory subunits to facilitate PKA activity (Chain et al., 1999). This effect was mostly examined *in vitro*, in *aplysia* sensory neurons (Chain et al., 1999) and nonneuronal mammalian cells (Dohrman et al., 1996). So whether a similar effect exists in mammalian neurons is unclear. Nonetheless, both CREB and the PKA regulatory subunits are possible targets quantifiable using the western blot technique already established in our lab.

To address the second focus, we may further examine the role inflammation has on the observed recovery after Rp treatment. We may also study the alternative cAMP activated target EPAC. This recently described cAMP target has two isoforms, EPAC1 and EPAC2, and the CNS specific EPAC2 may be involved in axon growth and guidance alongside PKA. For example, Boomkamp et al. (2014) demonstrated using a mixed rat spinal cord cell culture that damaged neurons extended greater number of neurites in the presence of rolipram and/or Rp compared to controls. The authors further reported a similar effect when they treated the mixed cultures with a specific agonist of EPAC, suggesting that it is cAMP activation of EPAC, and not PKA, that is

responsible for the neurite outgrowth. Along the same lines, Murray et al., (2009) reported that PKA inhibition in cultured embryonic rat spinal neurons led to growth cone attraction towards MAG, whereas silencing EPAC activity resulted in growth cone repulsion. In addition, Woolfrey et al. (2009) observed increased remodeling of neurite connections in healthy neurons resulting from EPAC activation. For the authors, this mechanism of EPAC was suggested to be responsible for certain CNS disorders that cause an inability to form stable neuronal connections. Within the context of SCI, increased synaptic remodeling and neurite attraction and outgrowth are processes required for adaptive changes and functional restoration to occur after the injury. As recent evidence suggests, EPAC may be just as central as PKA in mediating these effects, and thus may require greater attention in future research.

*e. Conclusions*

To address the contradictory results to our initial hypotheses, we posited that increased EPAC activation or inflammation resulting from PKA inhibition may be responsible for the observed recovery. Both (or neither) of these propositions may prove to be important with further experiments, yet the desire to delve deeper into the mechanisms of recovery after SCI is accompanied by a requirement of greater methodological knowledge on the part of researchers. Furthermore, researchers are also required to perform more complex and refined techniques to tease apart nuanced mechanisms. The current study planned for the use of a variety of arguably complicated biochemical and histological techniques to examine the effects of PKA inhibition on recovery. And as we laid out our experiments, we discovered that expertise in diverse fields such as cellular and molecular biology, pharmacology, etc, were required to satisfactorily perform our studies. This progress towards more complex studies may be address by the gradual increase in cooperative studies and team grants in the field. The potential of team grants allows us to explore the mechanisms of Rp mediated recovery in experiments that would be difficult for many single laboratories to perform. For example, we may evaluate the effect of EPAC activation on recovery both in animal models and *in vitro* cell cultures. *In vitro* experiments provide researchers with versatile means to examine how EPAC activation and inhibition affects neurite sprouting and the expression of growth promoting genes in a simpler environment. These experiments may be performed using combinations of pharmacological treatments and genetic transfection to manipulate PKA and EPAC activity and examine the effects on intact and damaged neurons, or in the presence of growth inhibitors such as myelin. *In vivo* experiments may be performed examining the effect of EPAC activation on behavioral recovery, and may be additionally compared to treatment groups that received Rp, rolipram, or no drug treatment. This would assess the relative efficacy of each of the cAMP signaling pathways on recovery after SCI, and may provide a new potential treatment for this debilitating injury.

The potential of cooperative studies to further progress in the field of recovery after SCI means that researchers may be much closer to their goal of ultimately increasing functional recovery for people suffering from the effects of SCI. But it may also be necessary to ask ourselves what purpose further mechanistic experiments serves towards achieving this goal, especially since we already observed increased recovery in this study with Rp treatment. While considering this question, it may be important to learn from the results of previous experiments, and examine how they ultimately contributed towards advancements in the field of SCI. A relevant example are studies examining the role the RST plays in CST rerouting. The RST is less important for motor control in humans as compared to rats, and the evidence for the RST contributing to motor recovery in humans is lacking. Nonetheless, the possibility of CST rerouting through the RST suggested the possibility that similar rerouting may occur in humans using tracts that are more essential for human motor control. For example, these possibilities are already being explored with other brainstem motor tracts, like the reticulospinal tract (reviewed in Nishimura & Isa, 2012). A second need for further mechanistic studies is to tease out biological factors truly important for recovery. The field of SCI is already littered with clinical trials that demonstrated promise in animal models, but frustratingly were not as effective in the human trials. Perhaps what was required, for at least a portion of these clinical trials, is the further exploration of mechanisms. For example, we may hypothetically observe, with additional experiments, that direct activation of EPAC is more effective for recovery than indirect activation resulting from PKA inhibition. Without further experiments, we may add another failed treatment to the pile and discard it as a dead end, when it had the potential to yield a much more promising treatment. The CNS is a complex system, and trying to repair it after injury is necessarily also complex. Only by attaining more detailed knowledge of how injury and recovery occurs through mechanistic studies are we likely to approach our goal of finding effective treatments for SCI.

## 5. References


Aglah C., Gordon, T., & Chavez, E.I.P. (2008). cAMP Promotes Neurite Outgrowth and Extension Through Protein Kinase A but Independently of Erk Activation in Cultured Rat Motoneurons. *Neuropharmacology, 55,* 8-17.

Allen, M. D., & Zhang, J. (2006). Subcellular Dynamics of Protein Kinase A Activity Visualized by FRET-Based Reporters. *Biochemical and Biophysical Research Communications, 348*, 716-721.

Anderson, K. D. (2004). Targeting Recovery: Priorities of the Spinal Cord-Injured Population. *Journal of Neurotrauma, 21*, 1371-1383.

Atkins, C. M., Olive Jr., A. A., Alonso, O. F., Pearse, D. D., Bramlett, H. M., Dietrich, W. D. (2007). Modulation of the cAMP Signaling Pathway after Traumatic Brain Injury. *Experimental Neurology, 208*, 145-158.

Bareyre, F. M., Kerschensteiner, M., Raineteau, O., Mettenleiter, T. C., Weinmann, O., & Schwab, M. E. (2004). The Injured Spinal Cord Spontaneously Forms a New Intraspinal Circuit in Adult Rats. *Nature Neuroscience, 7*, 269-277.

Beck, K. D., Nguyen, H. X., Galvan, M. D., Salazar, D. L., Woodruff, T. M., & Anderson, A. J. (2010). Quantitative Analysis of Cellular Inflammation after Traumatic Spinal Cord Injury: Evidence for a Multiphasic Inflammatory Response in the Acute to Chronic Environment. *Brain, 133*, 433-447.

Boomkamp, S. D., McGrath, M. A., Houslay, M. D., & Barnett, S. C. (2014). EPAC and the High Affinity Rolipram Binding Conformer of PDE4 Modulate Neurite Outgrowth and Myelination using an *in vitro* Spinal Cord Injury Model. *British Journal of Pharmacology, 171*, 2385-2398.

Borgens, R. B., & Liu-Snyder, P. (2012). Understanding Secondary Injury. *The Quarterly Review of Biology, 87,* 89-127.

Brus-Ramer, M., Carmel, J. B., Chakrabarty, S., & Martin, J. H. (2007). Electrical Stimulation of Spared Corticospinal Axons Augments Connections with Ipsilateral Spinal Motor Circuits after Injury. *The Journal of Neuroscience, 27*, 13793-13801.

Cafferty, W. B. J., Yang, S. H., Duffy, P. J., Li, S., & Strittmatter, S. M. (2007). Functional Axonal Regeneration through Astrocytic Scar Genetically Modified to Digest Chondroitin Sulfate Proteoglycans. *The Journal of Neuroscience, 27*, 2176-2185.

Cai, D., Qiu, J., Cao, Z., McAtee, M., Bregman, B. S., & Filbin, M. T. (2001). Neuronal Cyclic AMP Controls the Developmental Loss in Ability of Axons to Regenerate. *The Journal of Neuroscience, 21*, 4731-4739.

Cai, D., Shen, Y., De Bellard, M. E., Tang, S., & Filbin, M. T. (1999). Prior Exposure to Neurotrophins Blocks Inhibition of Axonal Regeneration by MAG and Myelin via a cAMP-Dependent Mechanism. *Neuron, 22*, 89-101.

Cao, Z., Gao, Y., Bryson, J.B., Hou, J., Chaudhry, N., Siddiq, M., Martinez, J., Spencer, T., Carmel, J., Hart, R.B., Filbin, M.T. (2006) The Cytokine Interleukin-6 is Sufficient but not Necessary to Mimic the Peripheral Conditioning Lesion Effect on Axonal Growth. *The Journal of Neuroscience, 26,* 5565-5573.

Chain, D. G., Casadio, A., Schacher, S., Hegde, A. N., Valbrun, M., Yamamoto, N., Goldberg, A. L., Bartsch, D., Kandel, E. R., & Schwartz, J. H. (1999). Mechanisms for Generating the Autonomous cAMP-Dependent Protein Kinase Required for Long-Term Facilitation in *Aplysia*. *Neuron, 22*, 147-156.

Chheda, M.G., Ashery, U., Thakur, P., Rettig, J., and Sheng, Z.H. (2001). Phosphorylation of Snapin by PKA Modulates its Interaction with the SNARE Complex. *Nature Cell Biology, 3,* 331-338.

Cohen, J. (1992). Statistical Power Analysis. *Current Directions in Psychological Science, 1,* 98-101.

David, S., & Kroner, A. (2011). Repertoire of Microglial and Macrophage Responses after Spinal Cord Injury. *Nature Reviews Neuroscience, 12*, 388-399.

Dohrman, D. P., Diamon, I., & Gordon, A. S. (1996). Ethanol Causes Translocation of cAMP-Dependent Protein Kinase Catalytic Subunits to the Nucleus. *PNAS, 93*, 10217-10221.

Donnelly, D. J., & Popovich, P. G. (2008). Inflammation and Its Role in Neuroprotection, Axonal Regeneration and Functional Recovery after Spinal Cord Injury. *Experimental Neurology, 209*, 378-388.

Esposito, M. S., Capelli, P., & Arber, S. (2014). Brainstem Nucleus MdV Mediates Skilled Forelimb Motor Tasks. *Nature, 508*, 351-356.

Filbin, M. T. (2003). Myelin-Associated Inhibitors of Axonal Regeneration in the Adult Mammalian CNS. *Nature Reviews Neuroscience, 4*, 1-11.

Fouad, K., Krajacic, A., & Tetzlaff, W. (2011). Spinal Cord Injury and Plasticity: Opportunities and Challenges. *Brain Research Bulletin, 84*, 337-342.

Fouad, K., Pedersen, V., Schwab, M. E., & Brosamle, C. (2001). Cervical Sprouting of Corticospinal Fibers after Thoracic Spinal Cord Injury Accompanies Shifts in Evoked Motor Responses. *Current Biology, 11*, 1766-1770.

Fouad, K., Schnell, L., Bunge, M. B., Schwab, M. E., Liebscher, T., & Pearse, D. D. (2005). Combining Schwann Cell Bridges and Olfactory-Ensheathing Glia Grafts with Chondroitinase Promotes Locomotor Recovery after Complete Transection of the Spinal Cord. *The Journal of Neuroscience, 25*, 1169-1178.

Fouad, K., & Tetzlaff, W. (2012). Rehabilitative Training and Plasticity Following Spinal Cord Injury. *Experimental Neurology, 235*, 91-99.

Gao, Y., Nikulina, E., Mellado, W., & Filbin, M. T. (2003). Neurotrophins Elevate cAMP to Reach a Threshold Required to Overcome Inhibition by MAG Through Extracellular Signal-Regulated

Kinase-Dependent Inhibition of Phosphodiesterase. *The Journal of Neuroscience, 23*, 11770-11777.

Garcia-Alias, G., Barkhuysen, S., Buckle, M., & Fawcett, J. W. (2009). Chondroitinase ABC Treatment Opens a Window of Opportunity for Task-Specific Rehabilitation. *Nature Neuroscience, 12*, 1145-1151.

Gervasi, N., Hepp, R., Tricoire, L., Zhang, J., Lambolez, B., Paupardin-Tritsch, D., & Vincent, P. (2007). Dynamics of Protein Kinase A Signaling at the Membrane, in the Cytosol, and in the Nucleus of Neurons in Mouse Brain Slices. *The Journal of Neuroscience, 27*, 2744-2750.

Girgis, J., Merrett, D., Kirkland, S., Metz, G. A. S., Verge, V., & Fouad, K. (2007). Reaching Training in Rats with Spinal Cord Injury Promotes Plasticity and Task Specific Recovery. *Brain, 130*, 2993-3003.

Gomez-Pinilla, F., Ying, Z., Roy, R. R., Molteni, R., & Edgerton, V. R. (2002). Voluntary Exercise Induces a BDNF-Mediated Mechanisms that Promotes Neuroplasticity. *Journal of Neurophysiology, 88*, 2187-2195.

Gonzalez, G. A., & Montminy, M. R. (1989). Cyclic AMP Stimulates Somatostatin Gene Transcription by Phosphorylation of CREB at Serine 133. *Cell, 59*, 675-680.

Hannila, S. S., & Filbin, M. T. (2008). The Role of Cyclic AMP Signalling in Promoting Axonal Regeneration after Spinal Cord Injury. *Experimental Neurology*, 209, 321-332

Harootunian, A. T., Adams, S. R., Wen, W., Meinkoth, J. L., Taylor, S. S., & Tsien, R. Y. (1993). Movement of the Free Catalytic Subunit of cAMP-Dependent Protein Kinase into and out of the Nucleus can be Explained by Diffusion. *Molecular Biology of the Cell, 4*, 993-1002.

Heffner, R., & Masterton, B. (1975). Variation in Form of the Pyramidal Tract and Its Relationship to Digital Dexterity. *Brain, Behavior and Evolution, 12*, 161-200.

Howe, A. K. (2004). Regulation of Actin-Based Cell Migration by cAMP/PKA. *Biochimica et Biophysica Acta, 1692*, 159-174.

Huber, A. B., Weimann, O., Brosamle, C., Oertle, T., & Schwab, M. E. (2002). Patterns of Nogo mRNA and Protein Expression in the Developing and Adult Rat and After CNS lesions. *The Journal of Neuroscience, 22*, 3553-3567.

Hurd, C., Weishaupt, N., & Fouad, K. (2013). Anatomical Correlates of Recovery in Single Pellet Reaching in Spinal Cord Injured Rats. *Experimental Neurology, 247,* 605-614.

Impey, S., Obrietan, K., Wong, S. T., Poser, S., Yano, S., Wayman, G., Deloulme, J. C., Chan, G., & Storm, D. R. (1998). Cross Talk between ERK and PKA is Required for $Ca^{2+}$ Stimulation of CREB-Dependent Transcription and ERK Nuclear Translocation. *Neuron, 21*, 869-883.

Isa, T., & Nishimura, Y. (2014). Plasticity for Recovery after Partial Spinal Cord Injury – Hierarchical Organization. *Neuroscience Research, 78*, 3-8.

Ito, D., Imai, Y., Ohsawa, K., Nakajima, K., Fukuuchi, Y., & Kohsaka, S. (1998). Microglia-Specific Localization of a Novel Calcium Binding Protein, IBA1. *Molecular Brain Research, 57*, 1-9.

Kanagal, S. G., & Muir, G. D. (2007). Bilateral Dorsal Funicular Lesions Alter Sensorimotor Behavior in Rats. *Experimental Neurology, 205*, 513-524.

Kigerl, K. A., Gensel, J. C., Ankeny, D. P., Alexander, J. K., Donnelly, D. J., & Popovich, P. G. (2009). Identification of Two Distinct Macrophage Subsets with Divergent Effects Cause either Neurotoxicity or Regeneration in the Injured Mouse Spinal Cord. *The Journal of Neuroscience, 29*, 13435-13444.

Kirkland, S. W., Coma, A. K., Colwell, K. L., Metz, G. A. S. (2008). Delayed Recovery and Exaggerated Infarct Size by Post-Lesion Stress in a Rat Model of Focal Cerebral Stroke. *Brain Research, 1201*, 151-160.

Krajacic, A., Ghosh, M., Puentes, R., Pearse, D. D., & Fouad, K. (2009). Advantages of Delaying the Onset of Rehabilitative Reaching Training in Rats with Incomplete Spinal Cord Injury. *European Journal of Neuroscience, 29*, 641-651.

Krajacic, A., Weishaupt, N., Girgis, J., Tetzlaff, W., & Fouad, K. (2010). Training-Induced Plasticity in Rats with Cervical Spinal Cord Injury: Effects and Side Effects. *Behavioral Brain Research, 214*, 323-331.

Kuchler, M., Fouad, K., Weinmann, O., Schwab, M. E., & Raineteau, O. (2002). Red Nucleus Projections to Distinct Motor Neurons Pools in the Rat Spinal Cord. *The Journal of Comparative Neurology, 448*, 349-359.

Lacroix, S., Havton, L. A., McKay, H., Yang, H., Brant, A., Roberts, J., & Tuszynski, M. H. (2004). Bilateral Corticospinal Projections Arise from Each Motor Cortex in the Macaque Monkey: A Quantitative Study. *The Journal of Comparative Neurology, 473*, 147-161.

Lemon, R. N. (2008). Descending Pathways in Motor Control. *Annual Review of Neuroscience, 31*, 195-218.

Lemon, R. N., & Griffiths, J. (2005). Comparing the Function of the Corticospinal System in Different Species: Organizational Differences for Motor Specialization? *Muscle & Nerve, 32*, 261-279.

MacDonald, E., Van der Lee, H., Pocock, D., Cole, C., Thomas, N., Vandenberg, P. M., Bourtchouladez, R., & Kleim, J. A. (2007). A Novel Phosphodiesterase Type 4 Inhibitor, HT-0712, Enhances Rehabilitation-Dependent Motor Recovery and Cortical Reorganization after Focal Cortical Ischemia. *Neurorehabilitation and Neural Repair, 21*, 486-496.

Maier, I. C., & Schwab, M. E. (2006). Sprouting, Regeneration and Circuit Formation in the Injured Spinal Cord: Factors and Activity. *Phil. Trans. R. Soc. B, 361*, 1611-1634.

Muir, G. D., Webb, A. A., Kanagal, S., & Taylor, L. (2007). Dorsolateral Spinal Injury Differentially Affects Forelimb and Hindlimb Action in Rats. *European Journal of Neuroscience, 25*, 1501-1510.

Murray, A. J. (2008). Pharmacological PKA Inhibition: All May Not be What it Seems. *Science Signaling, 1,* re4.

Murray, A. J., Tucker, S. J., & Shewan, D. A. (2009). cAMP-Dependent Axon Guidance is Distinctly Regulated by EPAC and Protein Kinase A. *The Journal of Neuroscience, 29*, 15434-15444.

Nathan, P. W. (1994). Effects on Movement of Surgical Incisions into the Human Spinal Cord. *Brain, 117,* 337-346.

Nikulina, E., Tidwell, J. L., Dai, H. N., Bregman, B. S., & Filbin, M. T. (2004). The Phosphodiesterase Inhibition Rolipram Delivered after a Spinal Cord Lesion Promote Axonal Regeneration and Functional Recovery. *PNAS, 101*, 8786-8790.

Nishimura, Y., & Isa, T. (2012). Cortical and Subcortical Compensatory Mechanisms after Spinal Cord Injury in Monkeys. *Experimental Neurology, 235*, 152-161.

Onifer, S. M., Smith, G. M., & Fouad, K. (2011). Plasticity after Spinal Cord Injury: Relevance to Recovery and Approaches to Facilitate It. *Neurotherapeutics, 8*, 283-293.

Pearse, D. D., Pereira, F. C., Marcillo, A. E., Bates, M. L., Berrocal, Y. A., Filbin, M. T., & Bunge, M. B. (2004). cAMP and Schwann Cells Promote Axonal Growth and Functional Recovery after Spinal Cord Injury. *Nature Medicine, 10*, 610-616.

Ploughman, M., Windle, V., MacLellan, C. L., White, N., Dore, J. J., & Corbett, D. (2009). Brain-Derived Neurotrophic Factor Contributes to Recovery of Skilled Reaching after Focal Ischemia in Rats. *Stroke, 40*, 1490-1495.

Punch, L. J., Self, D. W., Nestler, E. J., & Taylor, J. R. (1997). Opposite Modulation of Opiate Withdrawal Behaviors on Microfusion of a Protein Kinase A Inhibitor versus Activator into the Locus Ceruleus or Periaqueductal Gray. *Journal of Neuroscience, 17*, 8520-8527.

Raineteau, O., Fouad, K., Bareyre, F. M., & Schwab, M. E. (2002). Reorganization of Descending Motor Tracts in the Rat Spinal Cord. *European Journal of Neuroscience, 16*, 1761-1771.

Rapalino, O., Lazarov-Spiegler, O., Agranov, E., Velan, G. J., Yoles, E., Fraidakis, M., Solomon, A., Gepstein, R., Katz, A., Belkin, M., Hadani, M., & Schwartz, M. (1998). Implantation of Stimulated Homologous Macrophages Results in Partial Recovery of Paraplegic Rats. *Nature Medicine, 4*, 814-821.

Rooij, J., Zwartkruis, F. J. T., Verheijen, M. H. G., Cool, R. H., Nijman, S. M. B., Wittinghofer, A., & Bos, J. L. (1998). Epac is a Rap1 Guanine-Nucleotide-Exchange Factor Directly Activated by cyclic AMP. *Nature, 396,* 474-477.

Romero-Sandoval, A., Chai, N., Nutile-McMenemy, N., & DeLeo, J. A. (2008). A Comparison of Spinal IBA1 and GFAP Expression in Rodent Models of Acute and Chronic Pain. *Brain Research, 1219*, 116-126.

Sekhon, L. H. S., & Fehlings, M. G. (2001). Epidemiology, Demographics, and Pathophysiology of Acute Spinal Cord Injury. *Spine, 26*, S2-S12.

Sepe, M., Lignitto, L., Porpora, M., Donne, R. D., Rinaldi, L., Belgianni, G., Colucci, G., Cuomo, O., Viggiano, D., Scorziello, A., Garbi, C., Annunziato, L., & Feliciello, A. (2014). Proteolytic Control of Neurite Outgrowth Inhibitor Nogo-A by the cAMP/PKA Pathway. *PNAS, 111*, 15729-15734.

Simpson, L. A., Eng, J. J., Hsieh, J. T. C., Wolfe, D. L., & The Spinal Cord Injury Rehabilitation Evidence (SCIRE) Research Team. (2012). The Health and Life Priorities of Individuals with Spinal Cord Injury: A Systematic Review. *Journal of Neurotrauma, 29*, 1548-1555.

Song, H., Ming, G., He, Z., Lehmann, M., McKerracher, L., Tessier-Lavigne, M., & Poo, M. (1998). Conversion of Neuronal Growth Cone Responses from Repulsion to Attraction by Cyclic Nucleotides. *Science, 281*, 1515-1518.

Song, H., Ming, G., & Poo, M. (1997). cAMP-Induced Switching in Turning Direction of Nerve Growth Cones. *Nature, 388*, 275-279.

Sorrells, S. F., Caso, J. R., Munhoz, C. D., & Sapolsky, R. M. (2009). The Stressed CNS: When Glucocorticoids Aggravate Inflammation. *Neuron, 64*, 33-39.

Spinal Cord Injury (SCI) Facts and Figures at a Glance. (2014). *National Spinal Cord Injury Statistical Center.* Retrieved from https://www.nscisc.uab.edu/PublicDocuments/fact_figures_docs/Facts%202014.pdf

Starkey, M. L., Bleul, C., Maier, I. C., & Schwab, M. E. (2011). Rehabilitative Training Following Unilateral Pyramidotomy in Adult Rats Improves Forelimb Functions in a Non-Task-Specific Way. *Experimental Neurology, 232*, 81-89.

Steichen, J. M., Iyer, G. H., Li, S., Saldanha, S. A., Deal, M. S., Woods Jr., V. L., & Taylor, S. S. (2010). Global Consequences of Activation Loop Phosphorylation on Protein Kinase A. *The Journal of Biological Chemistry, 285*, 3825-3832.

Van den Berg, M. E. L., Castellote, J. M., Mahillo-Fernandez, I., & de Pedro-Cuesta, J. (2010). Incidence of Spinal Cord Injury Worldwide: A Systematic Review. *Neuroepidemiology, 34*, 184-192.

Vavrek, R., Girgis, J., Tetzlaff, W., Hiebert, G. W., & Fouad, K. (2006). BDNF Promotes Connections of Corticospinal Neurons onto Spared Descending Interneurons in Spinal Cord Injured Rats. *Brain, 129*, 1534-1545.

Vitolo, O. V., Sant'Angelo, A., Costanzo, V., Battaglia, F., Arancio, O., & Shelanski, M. (2002). Amyloid B-Peptide Inhibition of the PKA/CREB Pathway and Long-Term Potentiation: Reversibility by Drugs that Enhance cAMP Signaling. *PNAS, 99*, 13217-13221.

Wang, D., Ichiyama, R. M., Zhao, R., Andrews, M. R., & Fawcett, J. W. (2011). Chondroitinase Combined with Rehabilitation Promotes Recovery of Forelimb Function in Rats with Chronic Spinal Cord Injury. *The Journal of Neuroscience, 31*, 9332-9344.

Weidner, N., Ner, A., Salimi, N., & Tuszynski, M. H. (2001). Spontaneous Corticospinal Axonal Plasticity and Functional Recovery after Adult Central Nervous System Injury. *PNAS, 98*, 3513-3518.

Weishaupt, N., Hurd, C., Wei, D. Z., & Fouad, K. (2013). Reticulospinal Plasticity after Cervical Spinal Cord Injury in the Rat Involves Withdrawal of Projections Below the Injury. *Experimental Neurology, 247*, 241-249.

Westgren, N., & Levi, R. (1998). Quality of Life and Traumatic Spinal Cord Injury. *Arch Phys Med Rehabil, 79*, 1433-1439.

Whishaw, I. Q., Gorny, B., & Sarna, J. (1998). Paw and Limb Use in Skilled and Spontaneous Reaching after Pyramidal Tract, Red Nucleus and Combined Lesions in the Rat: Behavioral and Anatomical Dissociations. *Behavioral Brain Research, 93*, 167-183.

Woo, M. S., Jang, P. G., Park, J. S., Kim, W. K., Joh, T. H., & Kim, H. S. (2003). Selective Modulation of Lipopolysaccharide-Stimulated Cytokine Expression and Mitogen-Activated Protein Kinase Pathways by Dibutyryl-cAMP in BV2 Microglial Cells. *Molecular Brain Research, 113*, 86-96.

Woolfrey, K. M., Srivastava, D. P., Photowala, H., Yamashita, M., Barbolina, M. V., Cahill, M. E., Xie, Z., Jones, K. A., Quilliam, L. A., Prakriya, M., & Penzes, P. (2009). EPAC2 Induces Synapse Remodeling and Depression and Its Disease-Associated Forms Alter Spines. *Nature Neuroscience, 12*, 1275-1286.

Yang, H. W., & Lemon, R. N. (2003). An Electron Microscopic Examination of the Corticospinal Projection to the Cervical Spinal Cord in the Rat: Lack of Evidence for Cortico-Motoneuronal Synapse. *Experimental Brain research, 149*, 458-469.

Yoshikawa, M., Suzumura, A., Tamaru, T., Takayanagi, T., & Sawada, M. (1999). Effects of Phosphodiesterase Inhibitors on Cytokine Production by Microglia. *Multiple Sclerosis Journal, 5*, 126-133.

Z'Graggen, W. J., Fouad, K., Raineteau, O., Metz, G. A. S., Schwab, M. E., & Kartje, G. L. (2000). Compensatory Sprouting and Impulse Rerouting after Unilateral Pyramidal Tract Lesion in Neonatal Rats. *The Journal of Neuroscience, 20*, 6561-6569.

Zhou, L., & Shine, H. D. (2003). Neurotrophic Factors Expressed in both Cortex and Spinal Cord Induce Axonal Plasticity after Spinal Cord Injury. *Journal of Neuroscience Research, 74*, 221-226.